Core-to-Core Program

MEG II実験に向けたDLC-RPCの放射線照射による検出器への影響

高橋 真斗 (神戸大理)

家城 佳[A], 大谷 航[A], 大矢 淳史[A], 越智 敦彦, 恩田 理奈[A], 潘 晟[A], 山本 健介[A], 李 維遠[A] (神戸大学、 東京大学[A])

2023年2月19日 (日)
第29回 ICEPP シンポジウム

Outline

- **Introduction**
  - Charged lepton flavour violation
  - MEG II experiment
  - Radiative Decay counter for background suppression
  - Resistive Plate Chamber with Diamond-Like Carbon
- **Ageing of DLC-RPC**
  - Requirements of radiation-hardness
  - Radiation irradiation facilities
  - Results
- **Summary and prospects**

Outline

- **Introduction**
  - Charged lepton flavour violation
  - MEG II experiment
  - Radiative Decay counter for background suppression
  - Resistive Plate Chamber with Diamond-Like Carbon
- **Ageing of DLC-RPC**
  - Requirements of radiation-hardness
  - Radiation irradiation facilities
  - Results
- **Summary and prospects**

Charged Lepton Flavour Violation

- **In the Standard Model, lepton flavour is conserved**
- **Neutrino oscillation is observed**
  - Flavour in neutrino sector is violated
- **Charged Lepton Flavour Violation (cLFV)**
  - Practically never occurs in SM: $\mathcal{B}(\mu \to e\gamma) \sim 10^{-54}$
  - Many new physics predictions in a measurable region
    - SUSY-seasaw, SUSY-GUT etc.: $\mathcal{B}(\mu \to e\gamma) \sim \mathcal{O}(10^{-14})$

➡ **The discovery of cLFV is clear evidence of new physics**

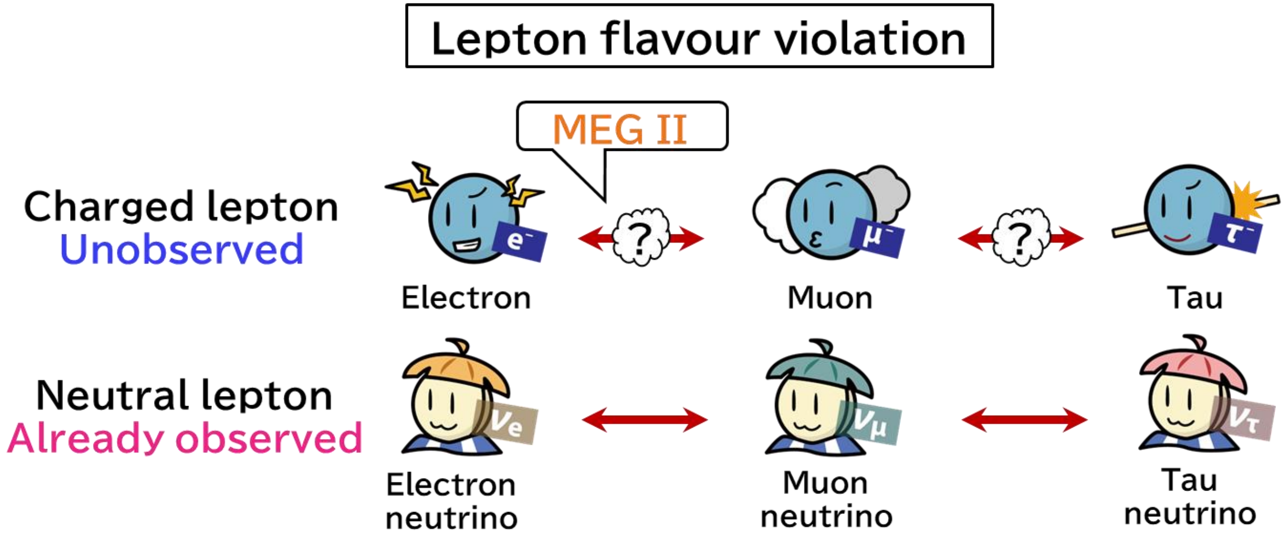

Ref) higgstan.com

MEG II experiment

$\mu^+ \to e^+\gamma$ search using the world's most intense μ^+ beam

- Upgraded from MEG experiment (2008 – 2013)
  - MEG result (2016): $\mathcal{B}(\mu^+ \to e^+\gamma) < 4.2 \times 10^{-13}$ (90% C.L.)

UTokyo
KEK
Kobe Uni.

PSI
ETHZ

INFN Genoa
INFN Lecce
INFN Pavia
INFN Pisa
INFN Roma

BINP
JINR

UC Irvine

~80 physicists

MEG

× 2 intensity μ^+ beam
× 2 resolution everywhere
× 2 efficiency

Upgrade !

MEG II

Search for $\mu^+ \to e^+\gamma$ down to

6×10^{-14} (90% C.L. sensitivity)

Physics run started from 2021 !!

$\mu^+ \to e^+\gamma$ signal and MEG II detectors

- **The $\mu^+ \to e^+\gamma$ signal features**
  - ✓ e^+ and γ have the same energy (52.8 MeV)
  - ✓ e^+ and γ emitted at the same time
  - ✓ e^+ and γ emitted in opposite directions

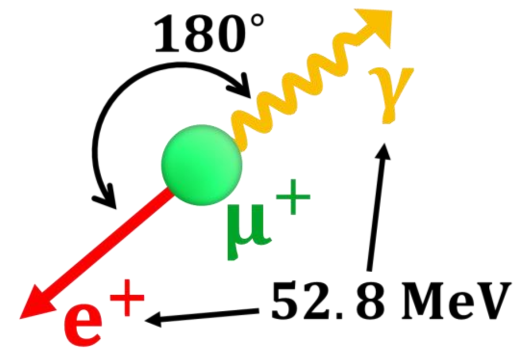

- **MEG II detectors**
  - γ detector
    - Liquid xenon calorimeter
  - e^+ detectors
    - Drift chamber
    - Timing counter

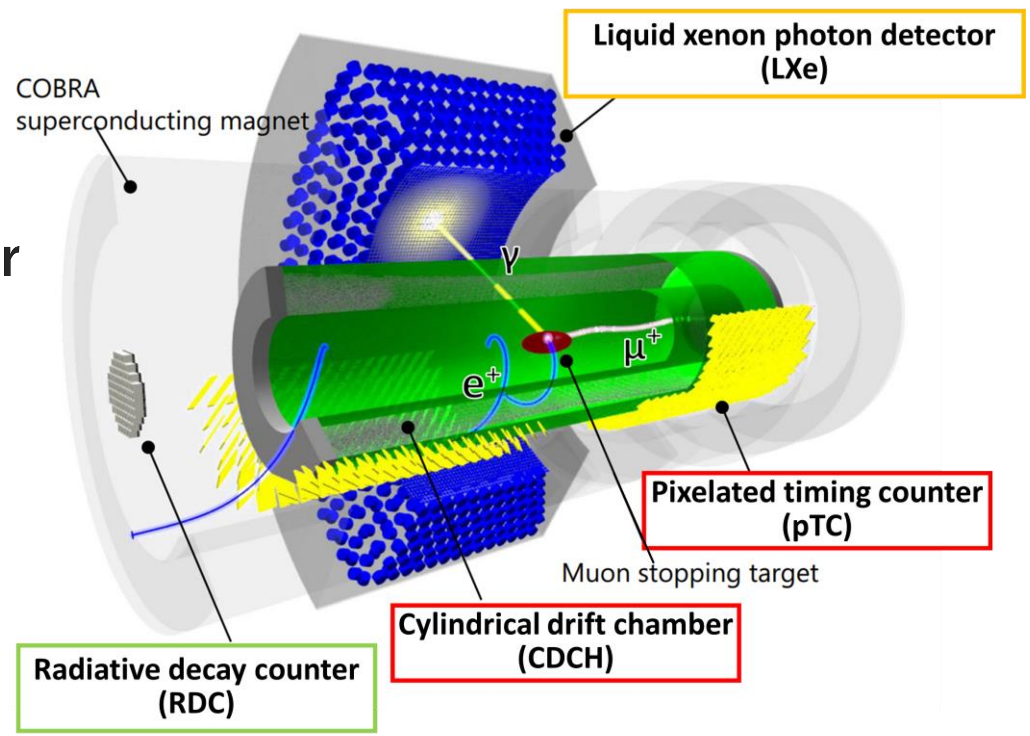

Background in MEG II

- **Accidental coincidence of BG-e^+ and BG-γ with different sources**
  - e^+ : Michel decay
  - γ : Radiative Muon Decay(RMD), Annihilation In Flight (AIF)

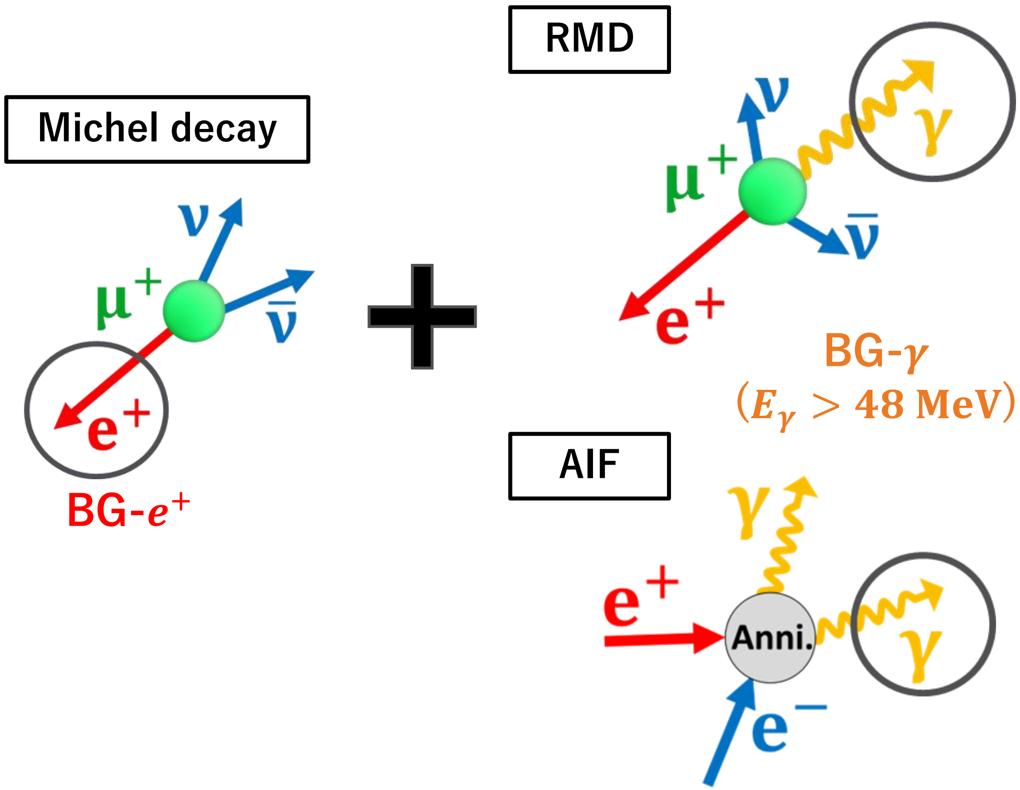

Sources of BG-γ ($E_\gamma > 48$ MeV)

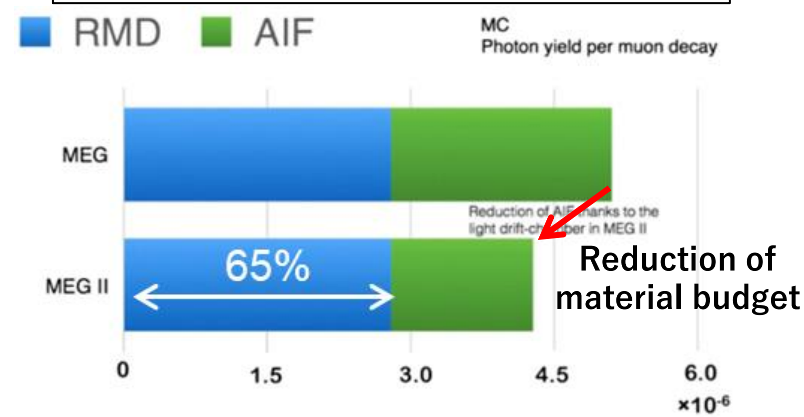

Identifying BG-γ with
Radiative Decay Counter (RDC)

Radiative Decay Counter (RDC)

- Detector for tagging BG-γ
- When BG-γ have signal-like energy $(\sim 52.8\ \mathrm{MeV})$ most of e^+ have a low energy $(1-5\ \mathrm{MeV})$
  - RMD e^+ distributed on the μ^+ beam axis

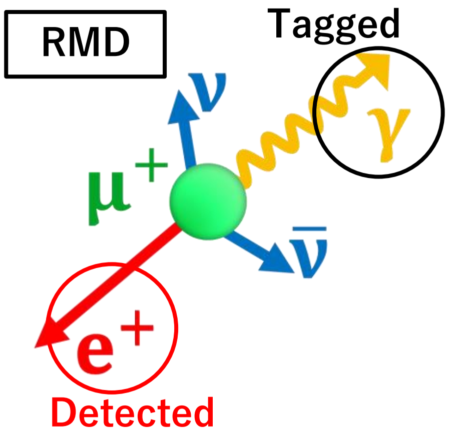

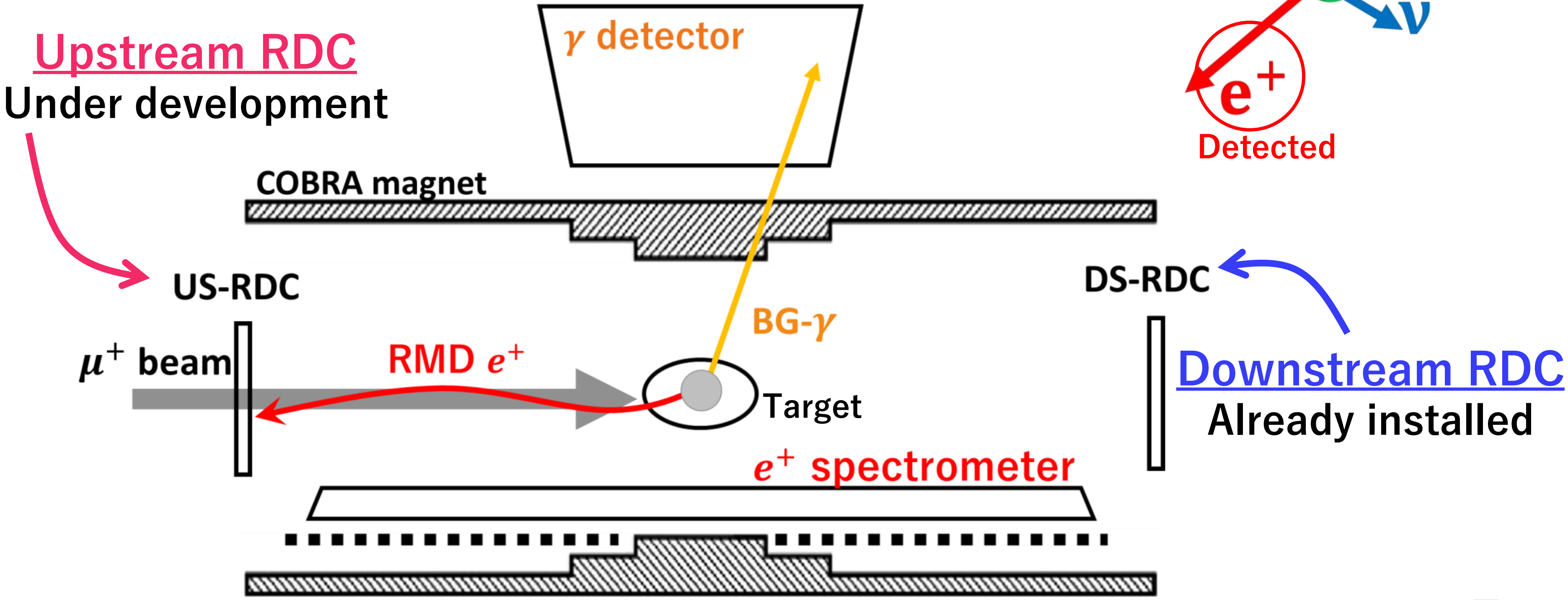

Requirements for upstream RDC

➢ US-RDC needs to detect MIP e^+ from RMD in a low-momentum and high-intensity muon beam
(28 MeV/c) $(1 \times 10^8\ \mu/s)$

1. Material budget: $< 0.1\%$ radiation length
2. Rate capability: $4\ \mathrm{MHz/cm^2}$ of muon beam
3. Radiation hardness: > 30 weeks operation
4. Efficiency: $> 90\%$ for MIP
5. Timing resolution: < 1 ns
6. Detector size: 20 cm (diameter)

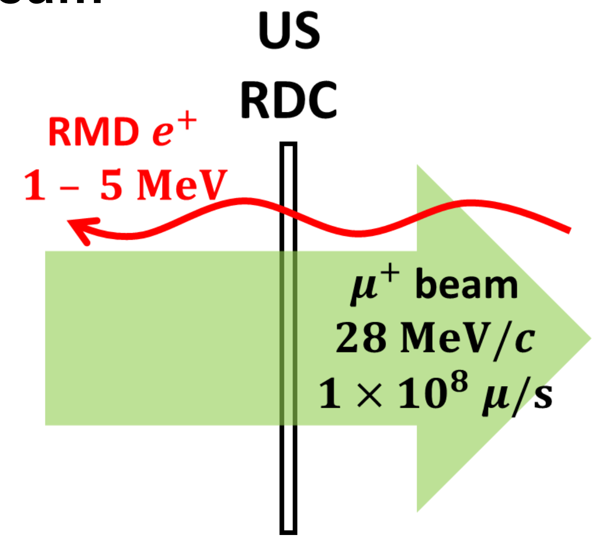

Developments of Resistive Plate Chamber (RPC) with Diamond-Like Carbon (DLC) electrodes for US-RDC

DLC-RPC

- DLC : high-resistance thin-film material
  - Small material budget by sputtering
  - Controllable resistivity by changing film thickness
- RPC : gas detector
  - Fast response (< 1 ns)
  - High detection efficiency (by multi layering)

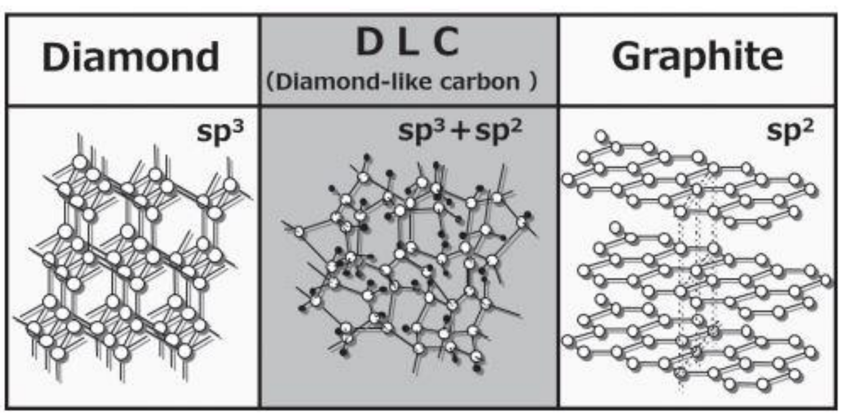

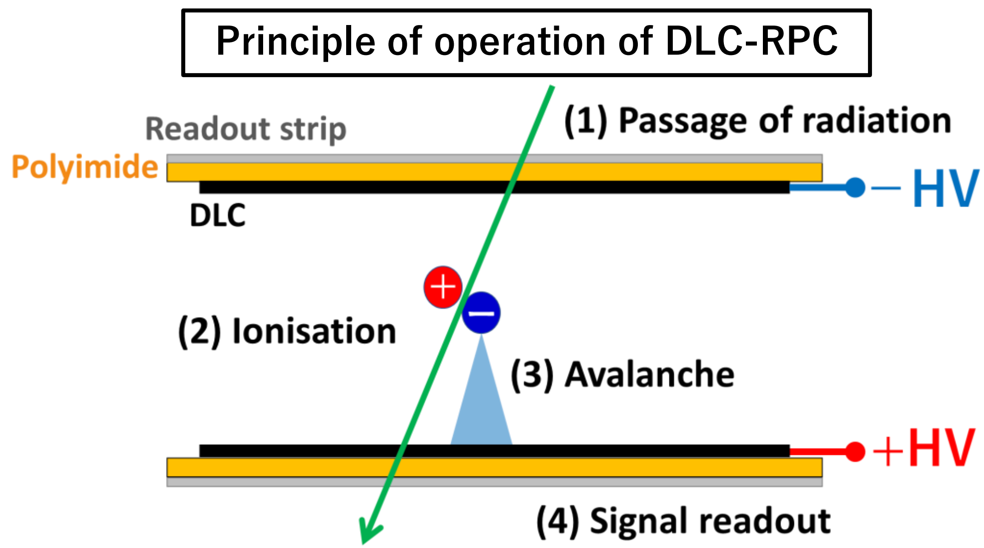

DLC-RPC for MEG II

DLC-RPC electrode sample

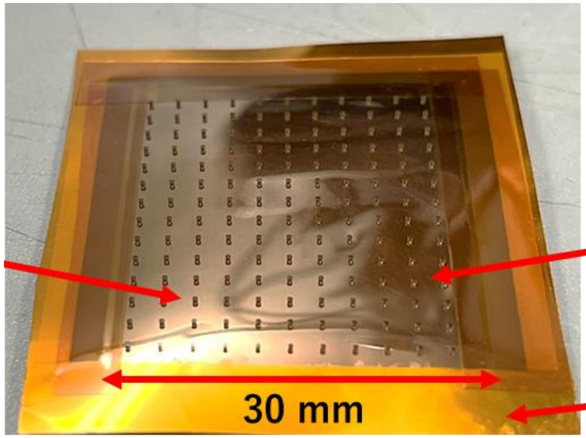

Scheme of MEG II DLC-RPC structure

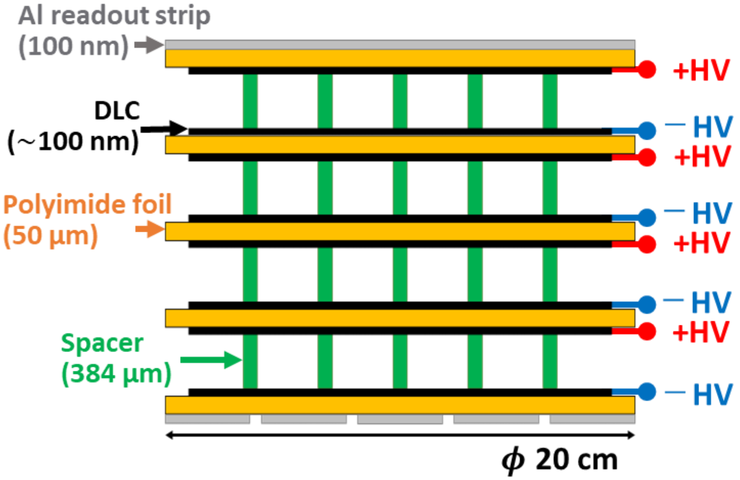

➢ Requirements for US-RDC and current status of DLC-RPC

Contents	Requirements	Current status
Material budget	$< 0.1\%\ X_0$	$\sim 0.095\%$
Rate capability	$4.0\ \mathrm{MHz/cm^2}$	$1\ \mathrm{MHz/cm^2}$
Radiation-hardness	> 30 weeks	N/A
Detection efficiency	$> 90\%$	$> 40\%$ (with single-layer), $> 90\%$ (calculated)
Timing resolution	1 ns	160 ps
Detector size	ϕ 20 cm	$3\ \mathrm{cm} \times 3\ \mathrm{cm}$ (active region)

Purpose of this study

- **Investigating radiation-hardness of DLC-RPC**
  - Radiation-hardness of DLC-RPC has not yet been studied
  - Known ageing effects in conventional RPC
    - Deposition on electrodes
    - Increased dark currents correlated to fluorine deposition

  ➔ We need to confirm in DLC-RPC as well

    - How much irradiation causes ageing?
    - Are there ageing specific to DLC-RPC?

- Li presents operation test and problems with the new electrode

Outline

- Introduction
  - Charged lepton flavour violation
  - MEG II experiment
  - Radiative Decay counter for background suppression
  - Resistive Plate Chamber with Diamond-Like Carbon
- Ageing of DLC-RPC
  - Requirements of radiation-hardness
  - Radiation irradiation facilities
  - Results
- Summary and prospects

Requirement for upstream RDC

- Requirement of radiation-hardness in MEG II experiment
  - 30 weeks operation in a low-momentum and high-rate μ^+ beam
    $28\ \mathrm{MeV}/c$ $4\ \mathrm{MHz/cm^2}$
  - Not easy to take out after installation

- Evaluation of ageing of DLC-RPC performance due to irradiation
  - The integrated charge due to irradiation is compared with the irradiation doses of μ^+ beam

- Estimation of irradiation doses in μ^+ beam
  - (Charge) = (Avalanche charge) × (Hit rate) × (Operational period)
    - Average avalanche charge：$3\ \mathrm{pC}$
    - Hit rate：$4\ \mathrm{MHz/cm^2}$

  ➔ $3\ \mathrm{pC} \times 4\ \mathrm{MHz/cm^2} \times 30\ \mathrm{weeks} \sim \mathcal{O}(100)\ \mathrm{C/cm^2}$

- **Irradiate as much as possible**

Irradiation facilities and test

- **Fast neutron radiation facility @Kobe Univ.**
  - 2022/6/20 – 2022/7/3
  - Tandem electrostatic accelerator
  - $^{9}\mathrm{Be} + \mathrm{d} \rightarrow {}^{10}\mathrm{B} + n + 4.36\ \mathrm{MeV}$
    - $\mathcal{O}(10^8)$ Neutron with peaks at 2.0 – 2.5 MeV

- **X-ray generator @KEK Platform-C**
  - 2022/8/29 – 2022/10/7
  - Cu target
    - X-ray with 8 keV

From these test,
Irradiation doses of $\mathcal{O}(100)\ \mathrm{mC/cm^2}$
were obtained

Setup of DLC-RPC

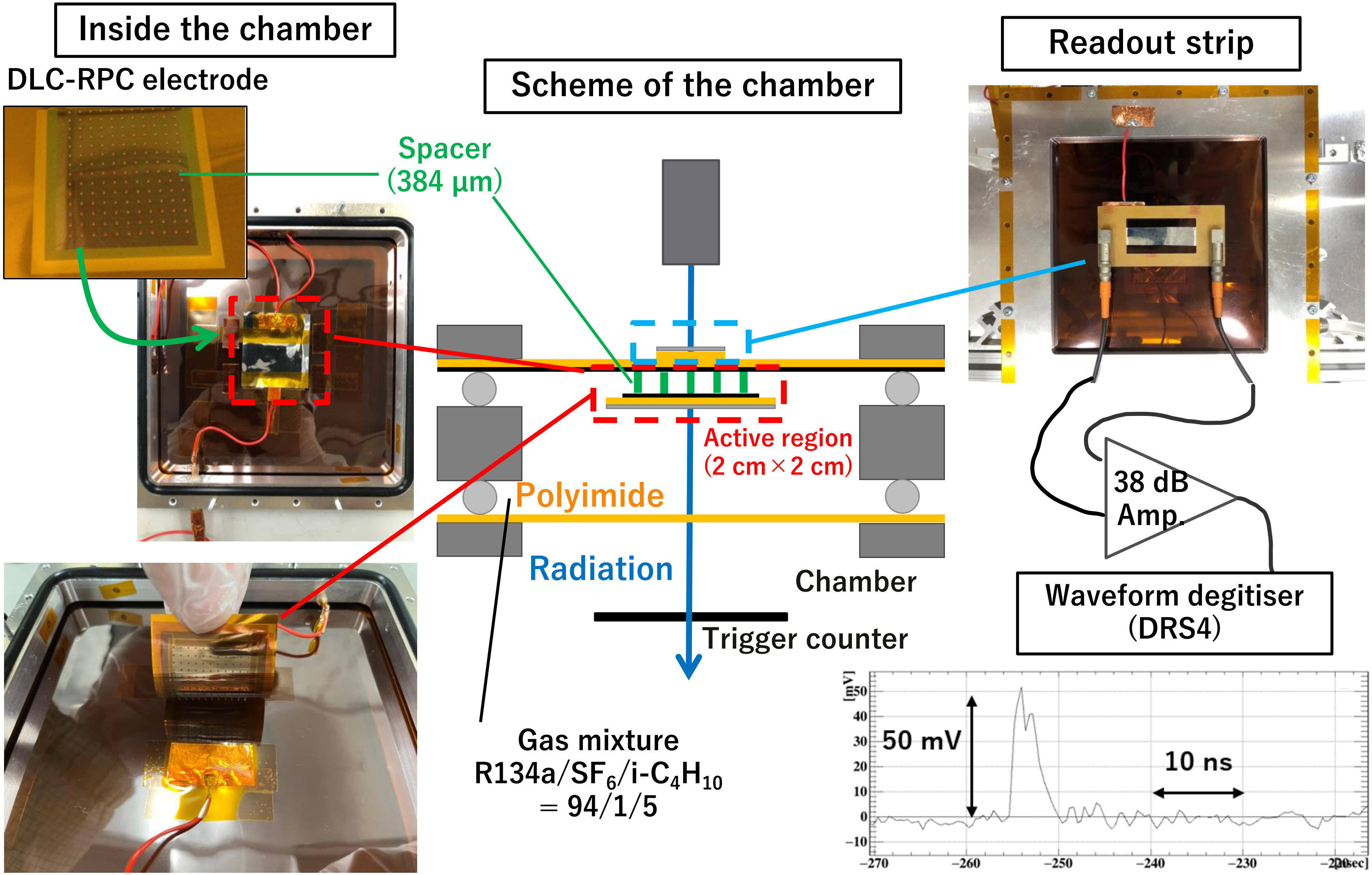

Setup of irradiation test

➢ **The chamber as close as possible to the output point**

Setup of neutron irradiation test

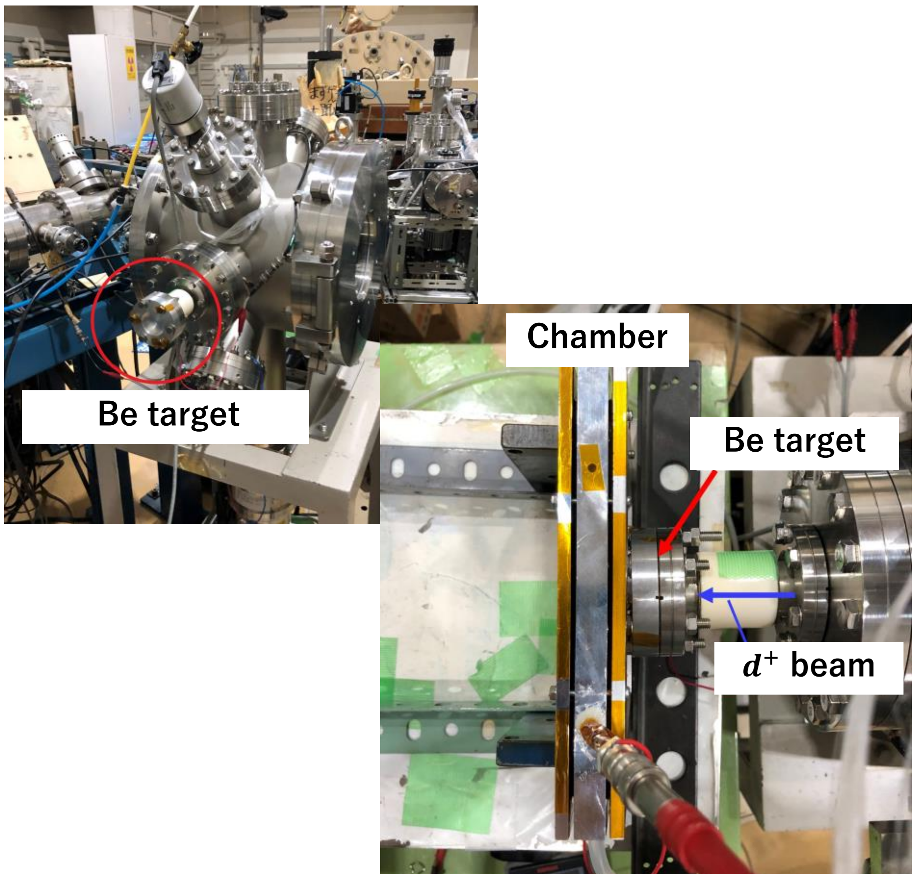

Setup of X-ray irradiation test

X-ray collimated to ϕ 1 cm

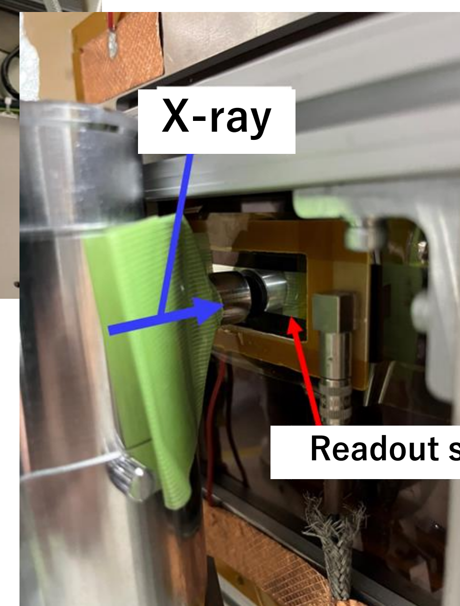

Results of total charge

- **Monitor detector current for irradiation dose evaluation**
  - Pulse height distributions for β-ray were measured to evaluation changes in performance of DLC-RPC due to irradiation
    - In addition, pulse height distributions for X-ray was measured continuously

Current during neutron irradiation

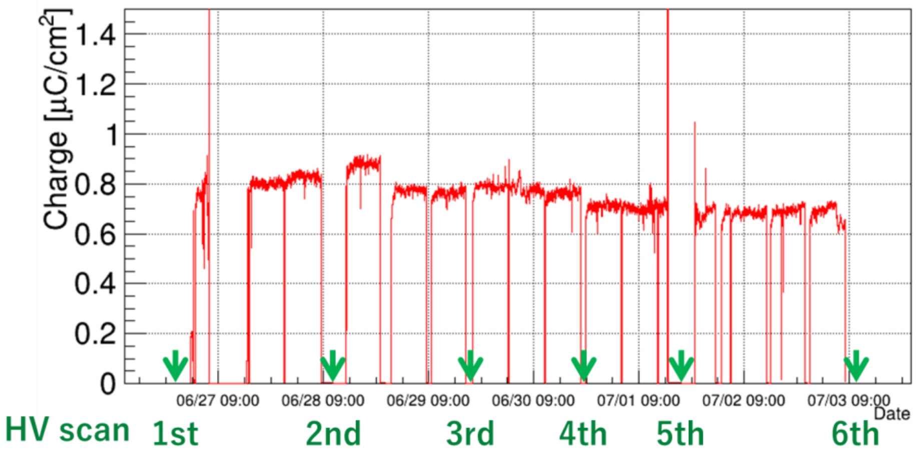

Current during X-ray irradiation

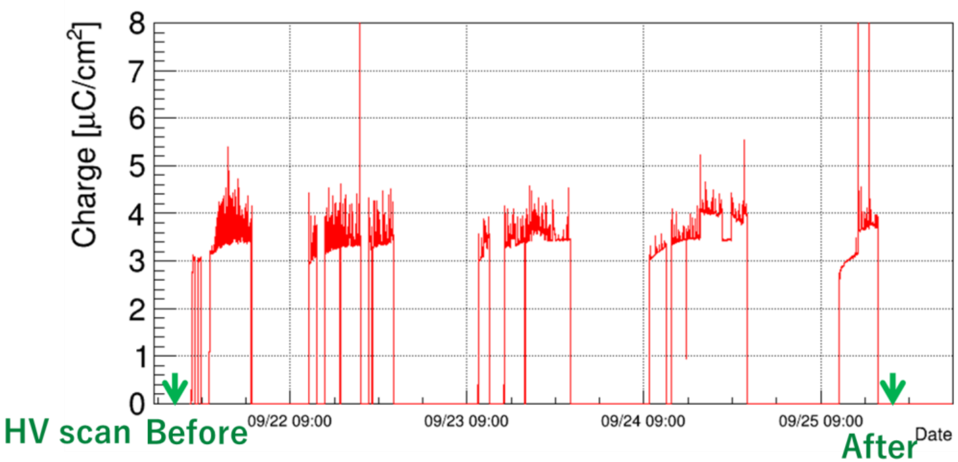

Total charge due to neutron irradiation
➔ 165 mC/cm^2

Total charge due to X-ray irradiation
➔ 272 mC/cm^2

Changes in performance of DLC-RPC

- **Neutron irradiation test**
  - 1st and 2nd, readout strip was not in place
  - Agreement at 6.4% from 3rd and 6th
- **X-ray irradiation test**
  - Agreement at 5.3% before and after irradiation

Pulse height distribution in neutron irradiation test @ 2750 V

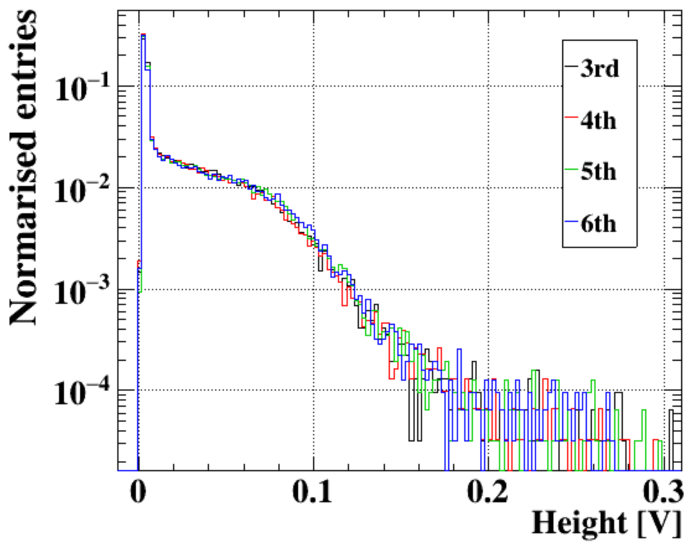

Pulse height distribution in X-ray irradiation test @ 2700 V

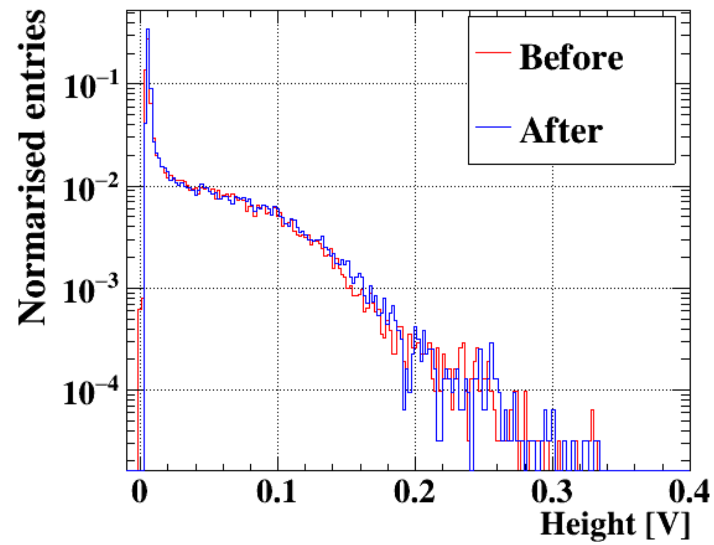

No significant ageing in performance DLC-RPC was observed at irradiation dose of $\mathcal{O}(100)\ \mathrm{mC/cm^2}$

Electrode surface condition survey

➢ Using X-ray Photoelectron Spectroscopy (XPS)

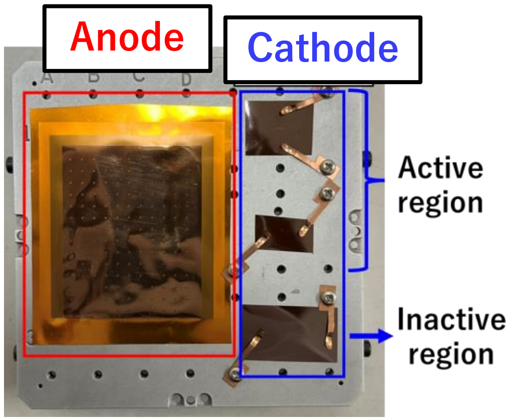

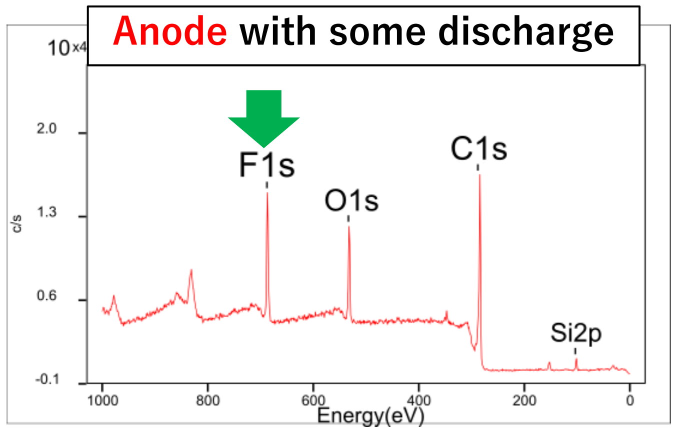

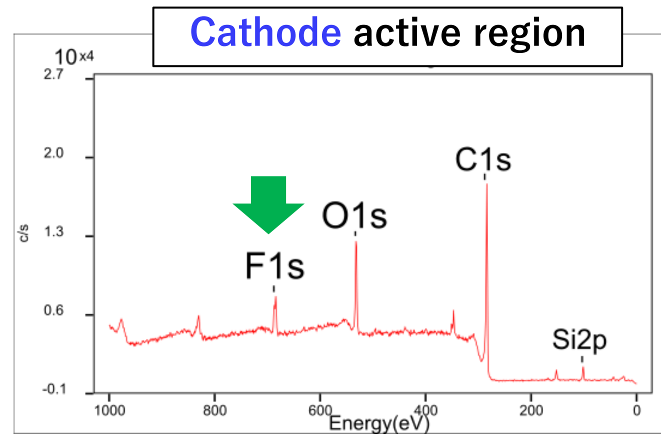

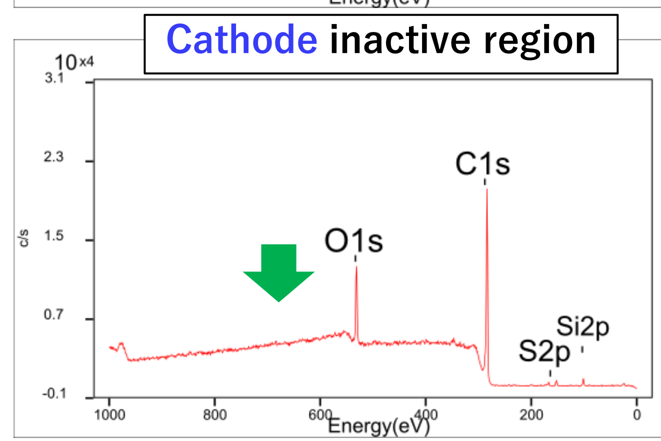

電極サンプル	C1s(%)	N1s(%)	O1s(%)	F1s(%)	Si2p(%)
Non-irradiation	79.03	3.19	17.78	–	–
Neutron irradiation （active region）	76.06	–	15.22	7.37	1.35
Neutron irradiation （inactive region）	72.82	3.02	19.72	1.53	2.91
X-ray irradiation （anode discharge point）	67.63	–	15.52	14.51	2.35
Cathode active region	74.82	–	17.22	5.89	3.68
Cathode inactive region	81.20	–	15.72	–	2.37

Ageing effect of DLC electrode

- **Fluorine deposition on electrode due to irradiation**
  - Proportional to the amount of charge generated
  - Fluorine does not deposit simply by being in contact with DLC-RPC gas
  - Ratio deposit to is higher for anode
- **Fluorine source is the operating gas of the DLC-RPC**
  - R134a ($C_2H_2F_4$): However, it is stable and hard to break a bond
  - SF_6: Generated during avalanche
    - $\mathbf{SF_6 + e^- \rightarrow SF_6^{-*}}, \quad \mathbf{SF_6^{-*} \rightarrow SF_5^- + F}$
- **Reports of the effects fluorine in other experiments**
  - Reported on Guida, R., RPC2022 and Rigoletti, G., RPC 2022.
  - Fluorine deposition and gas contamination cause dark currents

  ➔ Dark currents can be suppressed by quickly flowing polluted gases
    - Dark currents due to fluorine deposits on electrode are permanent

Outline

- Introduction
  - Charged lepton flavour violation
  - MEG II experiment
  - Radiative Decay counter for background suppression
  - Resistive Plate Chamber with Diamond-Like Carbon
- Ageing of DLC-RPC
  - Requirements of radiation-hardness
  - Radiation irradiation facilities
  - Results
- **Summary and prospects**

Summary

- DLC-RPC is under development for MEG II US-RDC
  - The low-momentum and high-intensity muon beam passage
    ➔ Several stringent requirements are imposed

- First study on the ageing of DLC-RPC
  - Using fast neutron and X-ray irradiation facility
  - $165\ \mathrm{mC/cm^2}$ integrated charge by fast neutron
  - $272\ \mathrm{mC/cm^2}$ integrated charge by X-ray with 8 keV
  - Integrated charge was 3 orders of magnitude lower than that of MEG II ($\mathcal{O}(100)\ \mathrm{C/cm^2}$)

- Ageing effect of DLC electrodes
  - Fluorine deposition on DLC electrodes

➔ <u>No significant ageing in performance was observed at this irradiation</u>

Prospects

➢ Further long-term irradiation

- Investigate whether detector performance deteriorates
- Effects of dark currents due to fluorine deposition
- Additional, long-term stable operation of the detector will be confirmed

➢ To reduce ageing due to fluorine

- Increased dark currents due to gas pollution reported by other experiments
  - Quick flowing polluted gas reduces dark currents

Backup

Charged lepton flavour violation

- **In the Standard Model, lepton flavour is conserved**
  - There is no explicit gauge symmetry
- **Neutrino oscillation have been observed**
  - Lepton flavour breaks between neutral leptons
  - Neutrinos have mass

ニュートリノ振動と$\mu \to e\gamma$崩壊

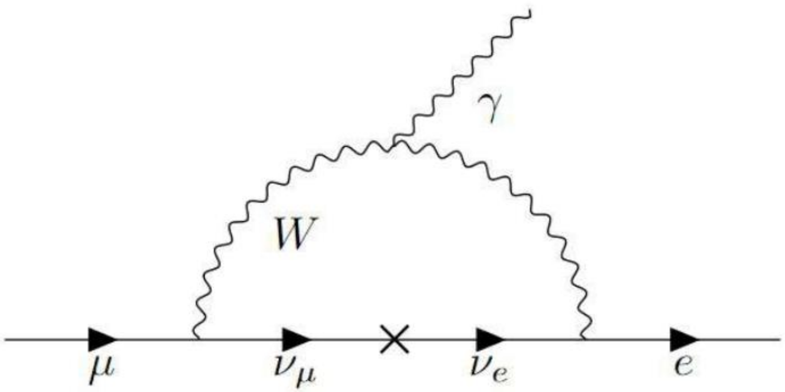

ニュートリノ振動を介した$\mu \to e\gamma$崩壊

$$\mathcal{B}(\mu \to e\gamma) = \frac{3\alpha}{32\pi}\left|\sum_{i=2,3} U^*_{\mu i} U_{ei} \frac{\Delta m^2_{i1}}{M^2_W}\right|^2 \sim 10^{-54}$$

α: 微細構造定数、U_{ij}: レプトン混合行列、Δm^2_{ij}: ニュートリノ質量の二乗差、M_W: ウィークボソンの質量

SUSYと$\mu \to e\gamma$崩壊

- **MSSM**
  - レプトンの質量行列を対角化した時、sleptonの質量行列の非対角成分は0でない
  - $\Delta m_{\tilde{\mu}\tilde{e}}$ によってsleptonのフレーバー混合によって$\mu \to e\gamma$崩壊が起こる
  - この時の$\mu \to e\gamma$崩壊分岐比は大きすぎる値が予想されている
  - LFVとFCNCの実験の制限から、SUSYの破れにはsleptonのフレーバー混合が抑制されなければならない
    ➔ 超対称フレーバー問題

- **$SU(5)$ SUSY-GUT**
  - 右巻きsleptonの質量行列の非対角成分によって$\mu \to e\gamma$崩壊が起こる
  - 右巻きsleptonのみが$\mu \to e\gamma$崩壊に寄与するため、生成される陽電子のヘリシティは左巻きが支配的
    ➔ $\mu^+ \to e_L^+\gamma$崩壊が支配的
  - sleptonの質量が数百 GeV/c^2 の時、崩壊分岐比$\mathcal{O}(10^{-14})$となる
  - 二つのヒッグスの真空期待値の比である$\tan\beta$ が大きい場合はさらに大きな崩壊分岐比が予想されている

- **$SO(10)$ SUSY-GUT**
  - 左巻きsleptonと右巻きsleptonの両方が$\mu \to e\gamma$崩壊に寄与
  - 崩壊分岐比は片方のヘリシティのみが寄与する場合と比べ$(m_\tau/m_\mu)^2$ で増大される

- **SUSY-seesaw**
  - 重い右巻きニュートリノをMSSMに導入
  - ニュートリノ混合が新たな湯川結合定数に起因すると仮定すると、
    ニュートリノ混合パラメータがsleptonの混合に影響し、$\mu \to e\gamma$崩壊分岐比を予想できる
  - 重い右巻きニュートリノの質量を$10^{10} - 10^{14}$ GeV/c^2 と仮定すると、SUSY-GUTと同程度の分岐比を予言する

MSSMと$\mu \rightarrow e\gamma$崩壊

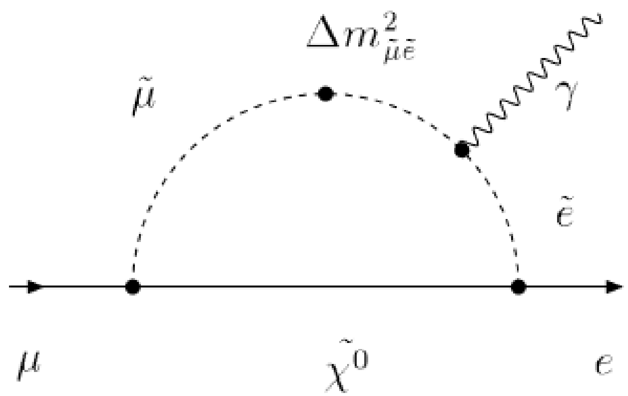

sleptonのフレーバ混合による$\mu \rightarrow e\gamma$崩壊

$SU(5)$ SUSY-GUTと$\mu \to e\gamma$崩壊

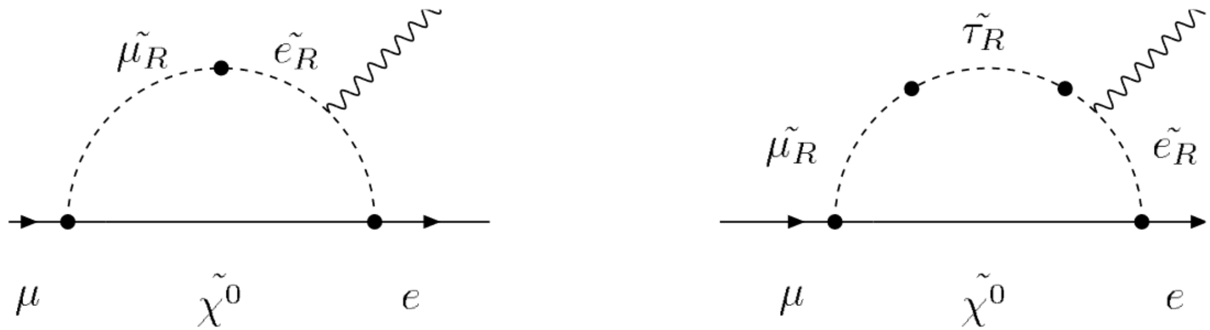

$SU(5)$ SUSY-GUTによる$\mu \to e\gamma$崩壊

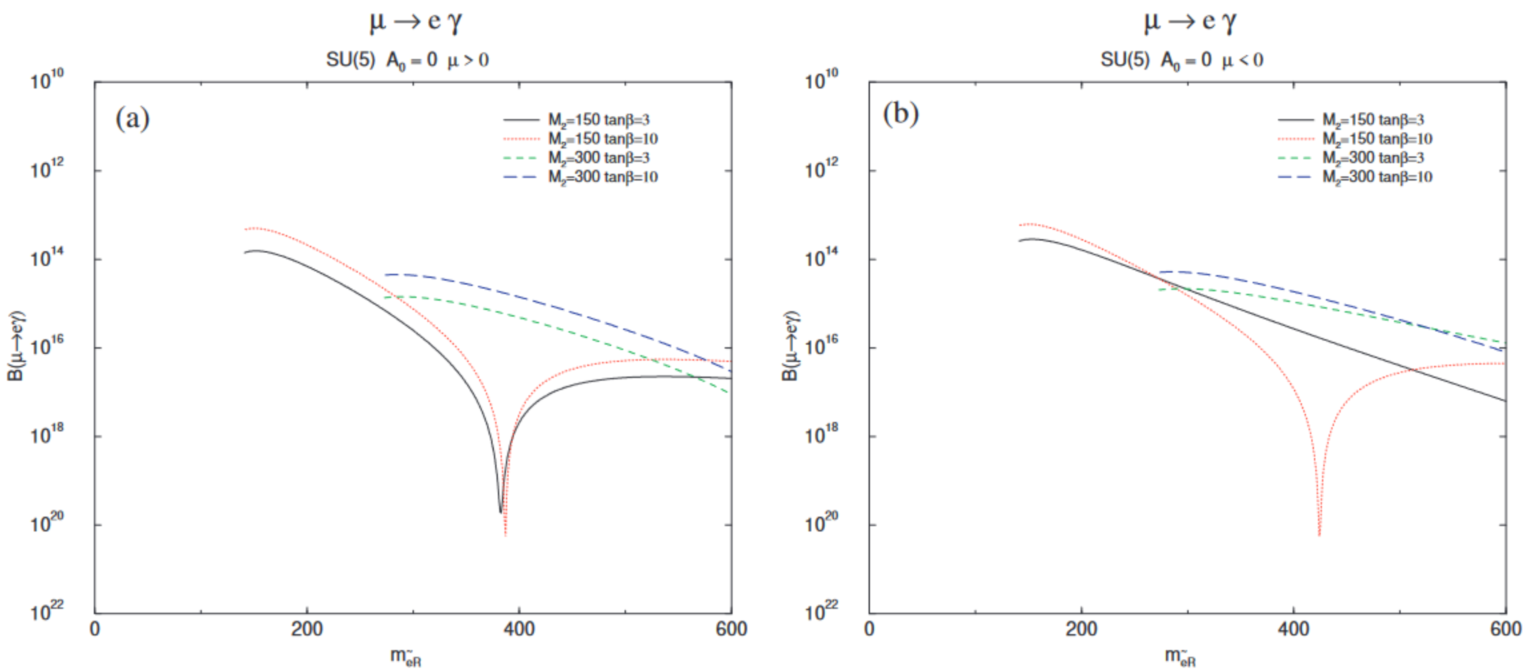

$SU(5)$ SUSY-GUTによる$\mu \to e\gamma$崩壊分岐比の例
横軸は右巻きsleptonの質量

$SO(10)$ SUSY-GUTと$\mu \to e\gamma$崩壊

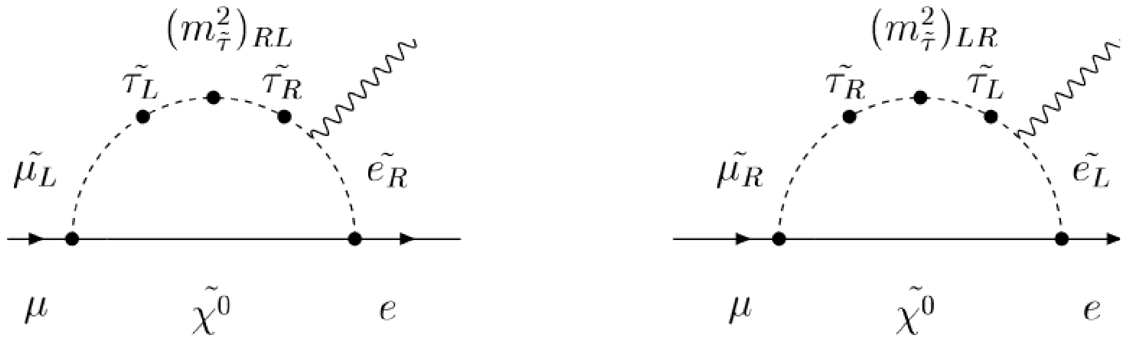

$SO(10)$ SUSY-GUTによる$\mu \to e\gamma$崩壊

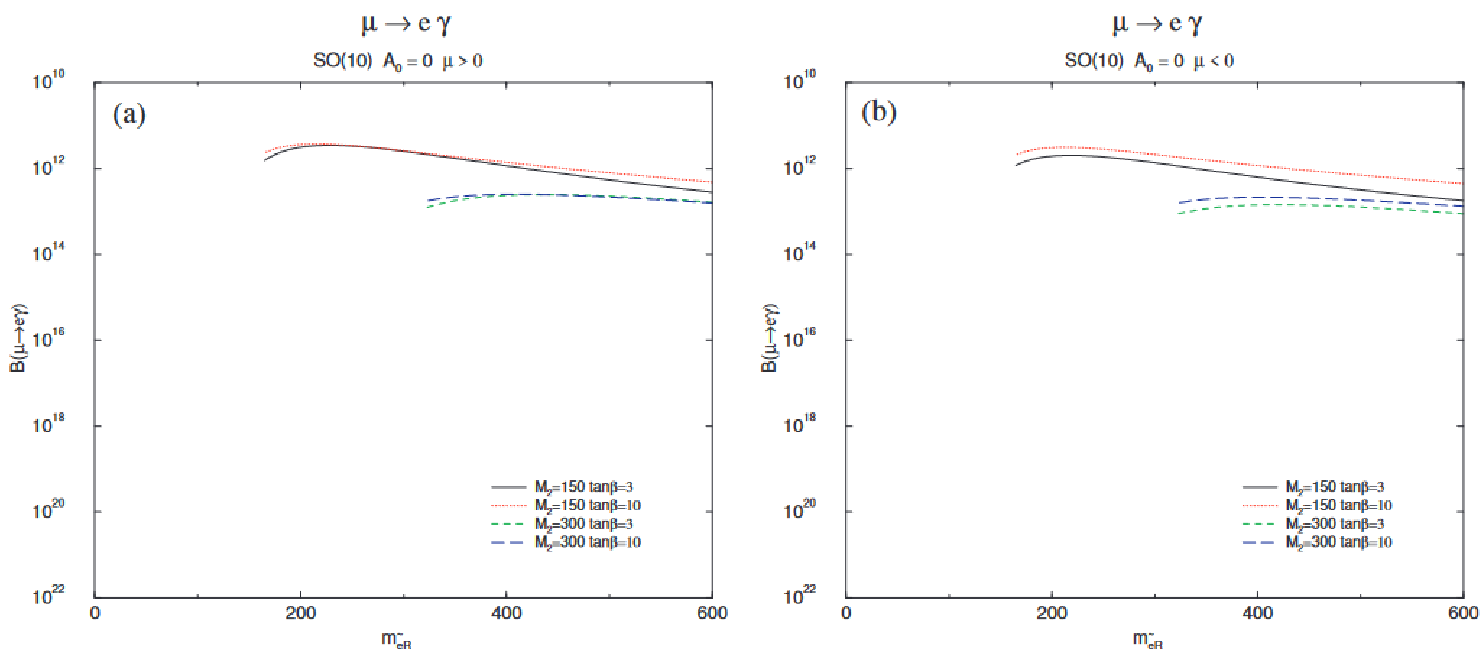

$SO(10)$ SUSY-GUTによる$\mu \to e\gamma$崩壊分岐比の例
横軸は右巻きsleptonの質量

SUSY-seesawと$\mu \to e\gamma$崩壊

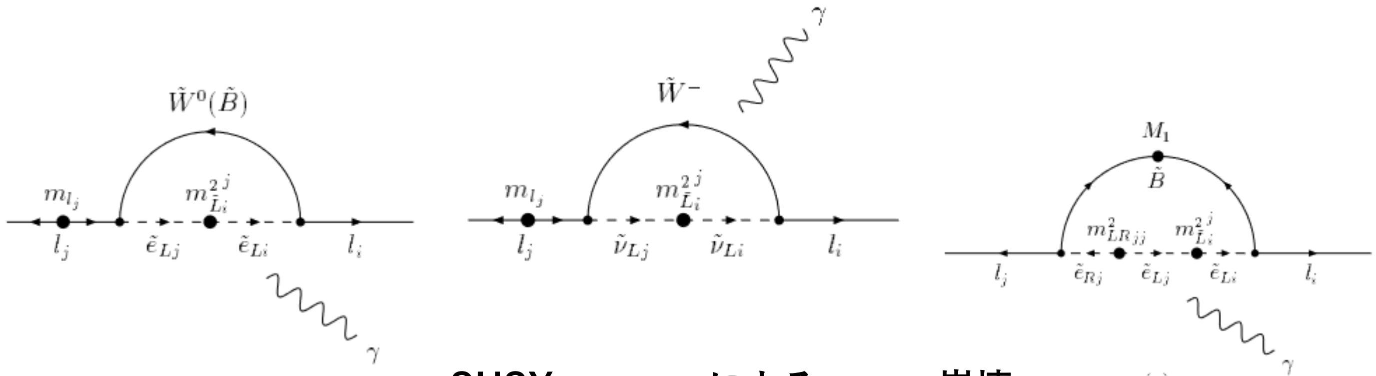

SUSY-seesawによる$\mu \to e\gamma$崩壊

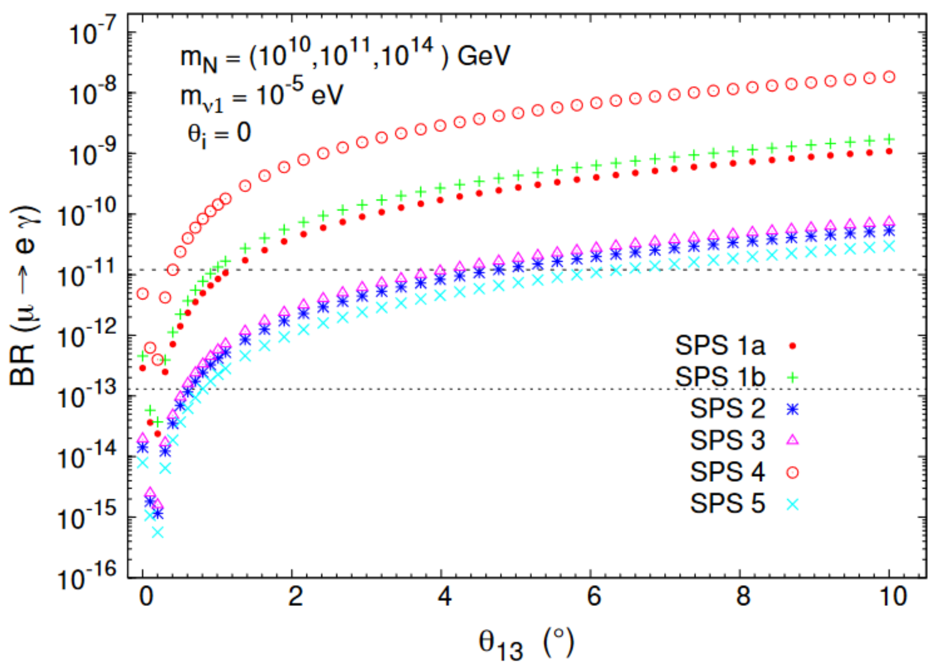

SUSY-seesawによる$\mu \to e\gamma$崩壊分岐比の例
横軸はニュートリノ質量の混合角θ_{13}

cLFVを伴うミューオンの崩壊探索最新結果

崩壊モード	崩壊分岐比の上限値（90% C.L.）
$\mu^+ \to e^+\gamma$	4.2×10^{-13} [3]
$\mu^+ \to e^+e^+e^-$	1.0×10^{-12} [23]
$\mu^+ \to e^+\gamma\gamma$	7.2×10^{-11} [24, 25]
$\mu^+ \to e^+\nu_\mu\bar{\nu}_e$	1.2×10^{-2} [26]
$\mu^-\mathrm{Au} \to e^-\mathrm{Au}$	7×10^{-13} [27]
$\mu^+e^- \times \mu^-e^-$	8.3×10^{-11} [28]

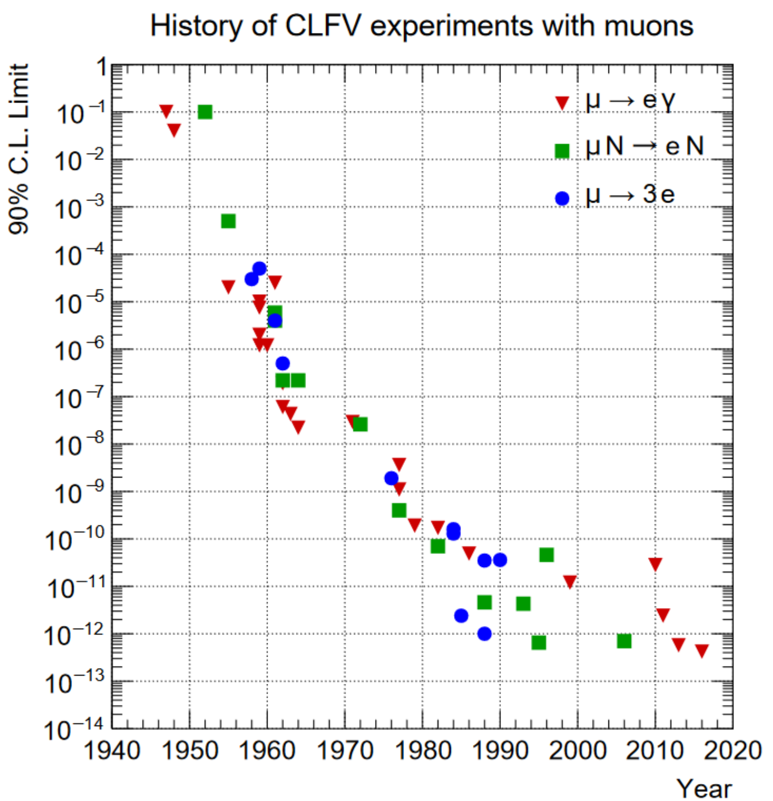

[3] Baldini, A. M., “Search for the lepton flavour violating decay $\mu^+ \to e^+\gamma$ with the full dataset of the MEG experiment”, The European Physical Journal C 76 (2016)

[23] Bellgardt, U. et al., “Search for the decay $\mu^+ \to e^+\gamma$”, Nuclear Physics B 618 (2001)

[24] Bolton, R. D. et al., “Search for rare muon decays with the Crystal Box detector”, Phys. Rev. D 38 (1988)

[25] Grosnick, D. et al., “Search for the rare decay $\mu^+ \to e^+\gamma\gamma$”, Phys. Rev. Lett. 57 (1986)

[26] Freedman, S. J. et al., “Limits on neutrino oscillations from $\overline{\nu}_e$ appearance”, Phys. Rev. D 47 (1993)

[27] The SINDRUM II Collaboration, “A search for $\mu - e$ conversion in muonic gold”, Eur. Phys. J. C.

[28] Willmann, L. et al., “New Bounds from a Search for Muonium to Antimuonium Conversion”, Phys. Rev. Lett 82 (1999)

MEG II実験における偶発的背景事象のエネルギー分布

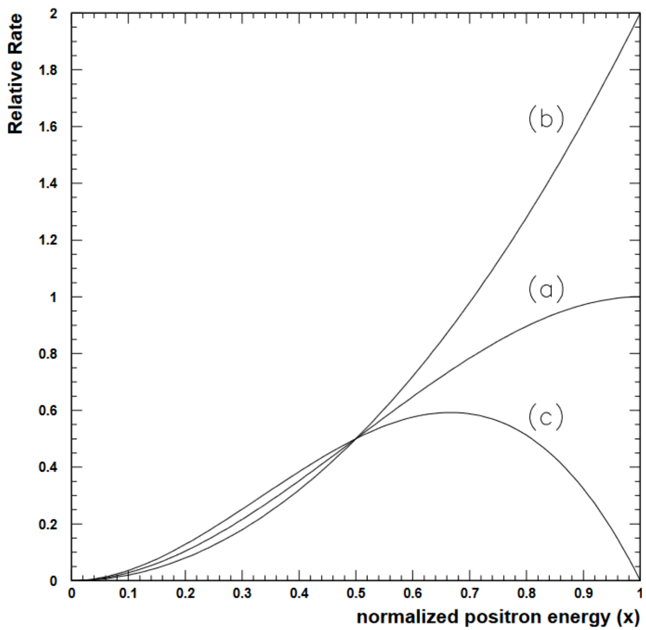

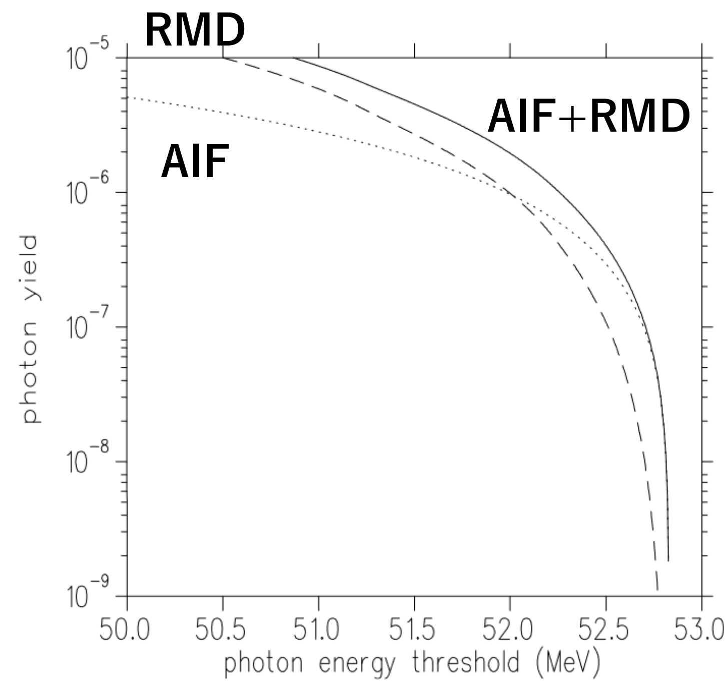

- **Michel陽電子**
  - 100%偏極したμ^+
  - 微分崩壊分岐比は

$$\frac{d^2\Gamma(\mu^\pm \to e^\pm \nu\bar{\nu})}{dx d\cos\theta_e} = \frac{m_\mu^5 G_F^2}{192\pi^3} x^2 \left[(3-2x) \pm P_\mu \cos\theta_e (2x-1)\right]$$

- **背景ガンマ線**

COBRA電磁石

A)

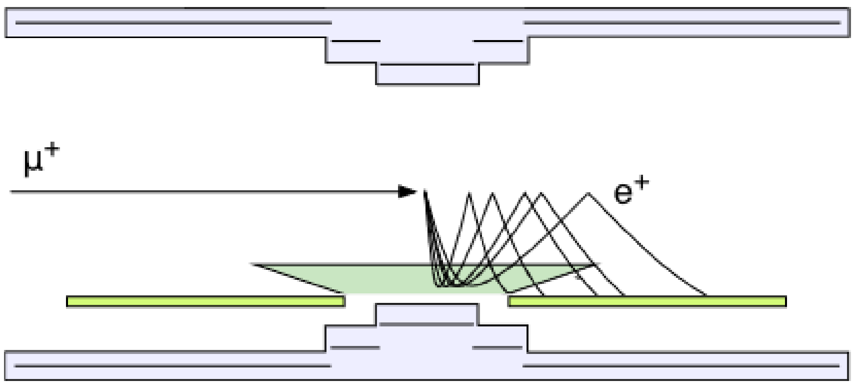

B)

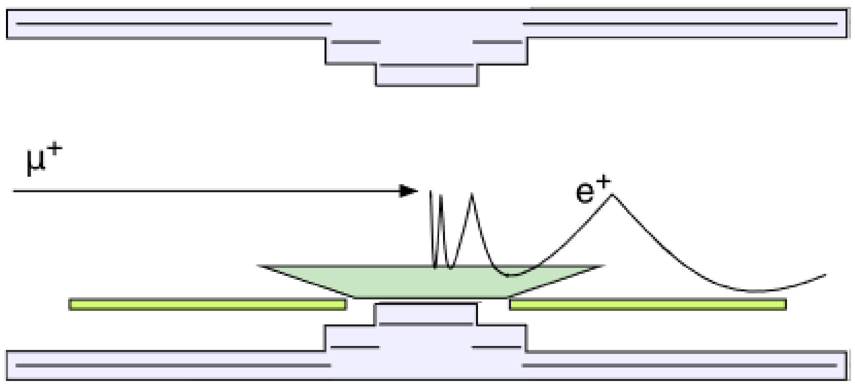

COBRA電磁石の形成する勾配磁場の概念
検出器模式図はMEG実験時のもの

- 勾配磁場を持つ COnstant Bending RAdius 電磁石
  - A） 信号領域付近のエネルギーを持つ陽電子が放出角に依らず、一定の回転半径を持って運動
  - B） μ^+ビーム軸に垂直に放出された陽電子が検出層から素早く排出

下流側RDC

- 前方に時間測定用のプラスチックシンチレータ
- 後方にエネルギー測定用のLYSO結晶

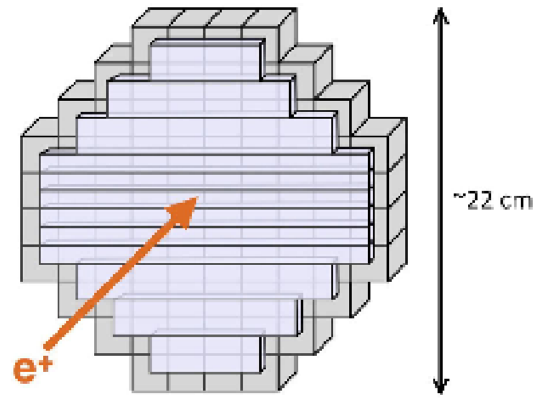

下流側RDCでの陽電子検出とLxeでのガンマ線検出の時間差

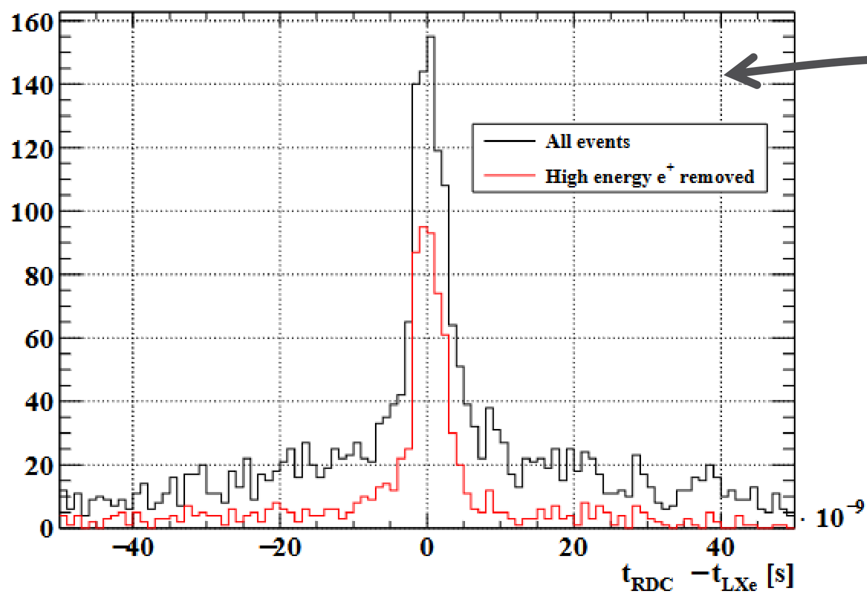

RDCの位置での陽電子のエネルギー

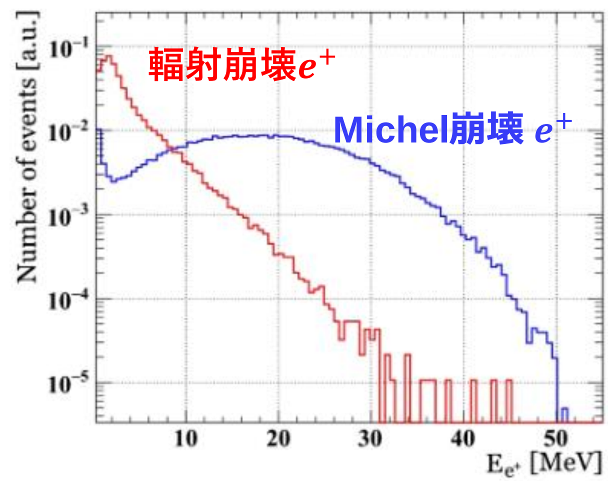

MEG II実験の検出器性能

	MEG 実験	MEG II design	MEG II updated
e^+ の運動量分解能 $\sigma_{p_{e^+}}$ (keV/c)	380	130	100
e^+ の角度分解能 $\sigma_{\theta_{e^+}}$ (mrad)	9.4	5.3	6.7
γ のエネルギー分解能 σ_{E_γ} (%) $(w < 2$ cm$)/(w > 2$ cm$)$	2.4 / 1.7	1.1 / 1.0	1.7 / 1.7
γ の位置分解能 σ_{x_γ} (mm)	5	2.4	2.4
e^+ と γ の時間分解能 $\sigma_{t_{e^+\gamma}}$ (ps)	122	84	70
e^+ の検出効率 ϵ_{e^+} (%)	30	70	65
γ の検出効率 ϵ_γ (%)	63	69	69

➢ **Baldini, A. M. et al., "The Search for $\mu^+ \rightarrow e^+\gamma$ with 10^{14} Sensitivity: The Upgrade of the MEG II Experiment", Symmetry 13 (2021)**

MEG II実験で予想される探索感度

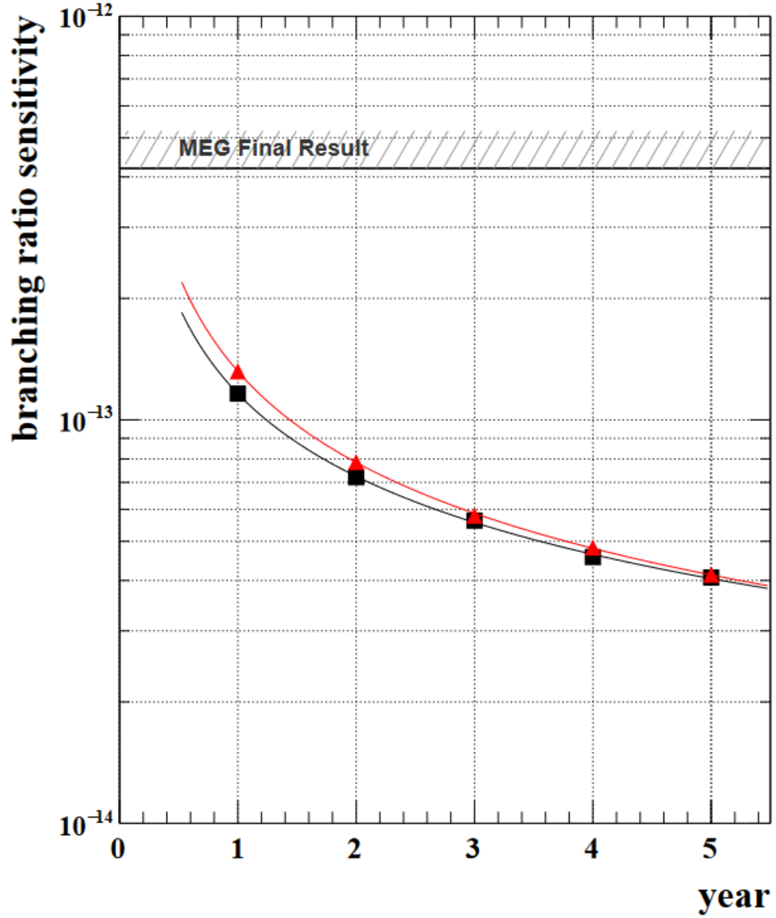

- 上流側RDCの寄与は含んでいない
  - Onda, R., “Suppression of γ-ray background for the highest sensitivity of $\mu^+ \to e^+\gamma$ search in MEG II experiment”, Ph. D. dissertation, The University of Tokyo (2021) により計算

μ^+ビームとRMD e^+ の分布

- MCより、どちらも中心付近に多い分布

  ➔ 検出器中心に孔を空けることはできない

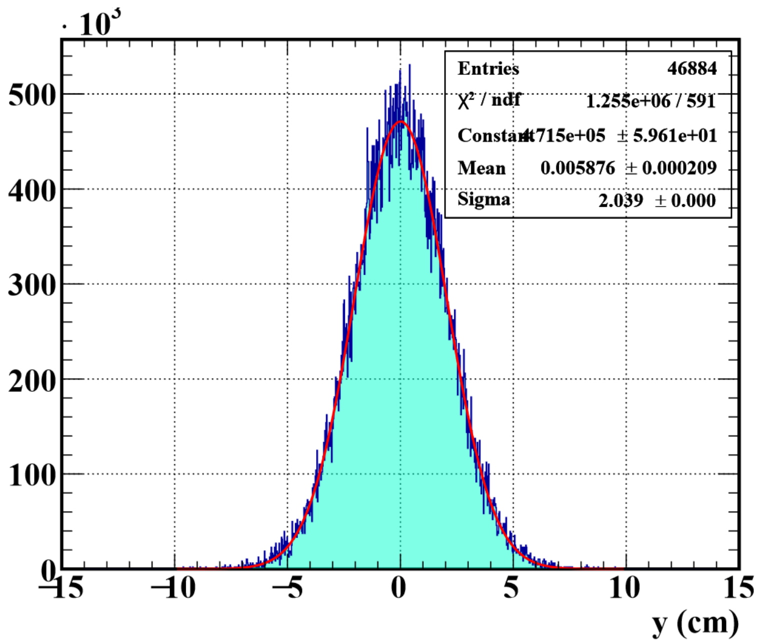

μ^+ビーム ($\sigma = 2.0$ cm)

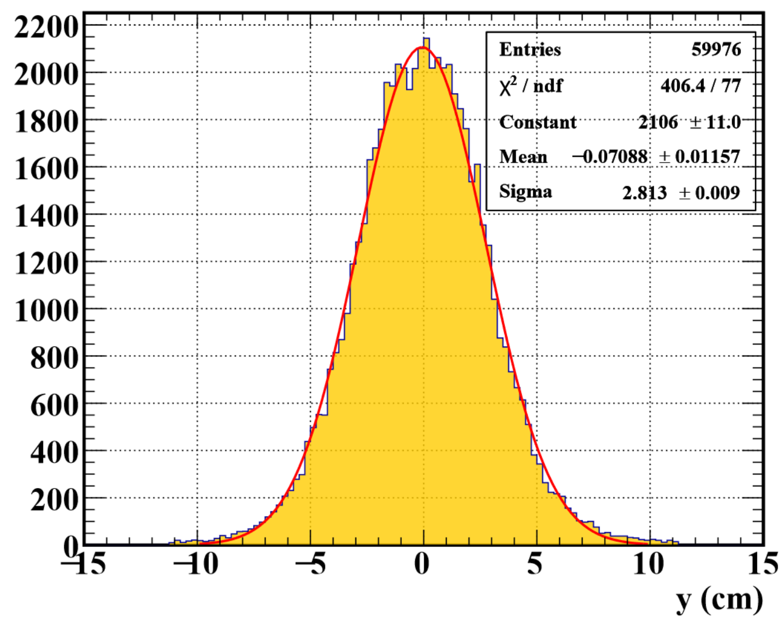

RMD e^+ ($\sigma = 2.8$ cm)

従来型のResistive Plate Chamber

- 高抵抗電極にはガラスが用いられることが多い
  - ガラスの体積抵抗率は一般的には $10^{13}\ \Omega\mathrm{cm}$
    - 酸化物の添加により $10^{8} - 10^{9}\ \Omega\mathrm{cm}$
    - この場合のレート耐性は $100\ \mathrm{kHz/cm^2}$ まで報告されている
(Liu, Z. et al., NIM A 959 (2020))

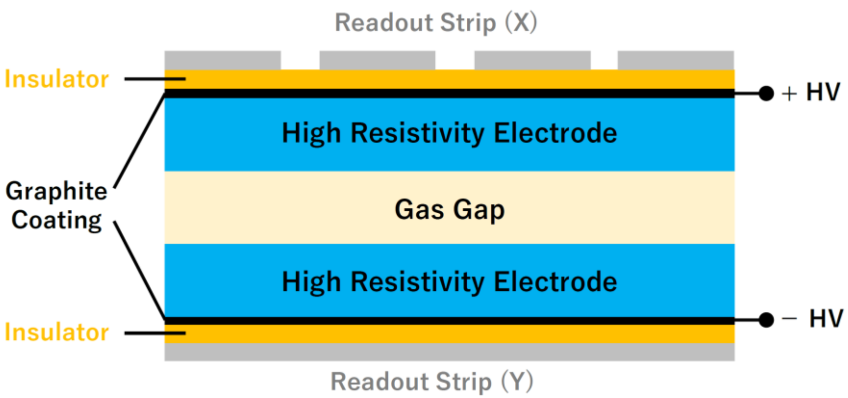

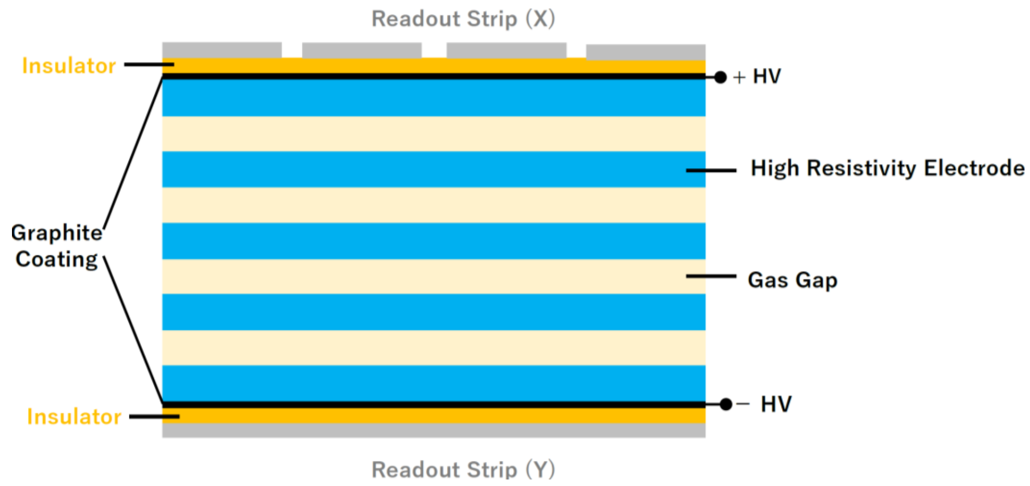

空間電荷効果

➢ $\mathbf{10^7 - 10^8}$ 程度の増幅率で増幅が飽和する

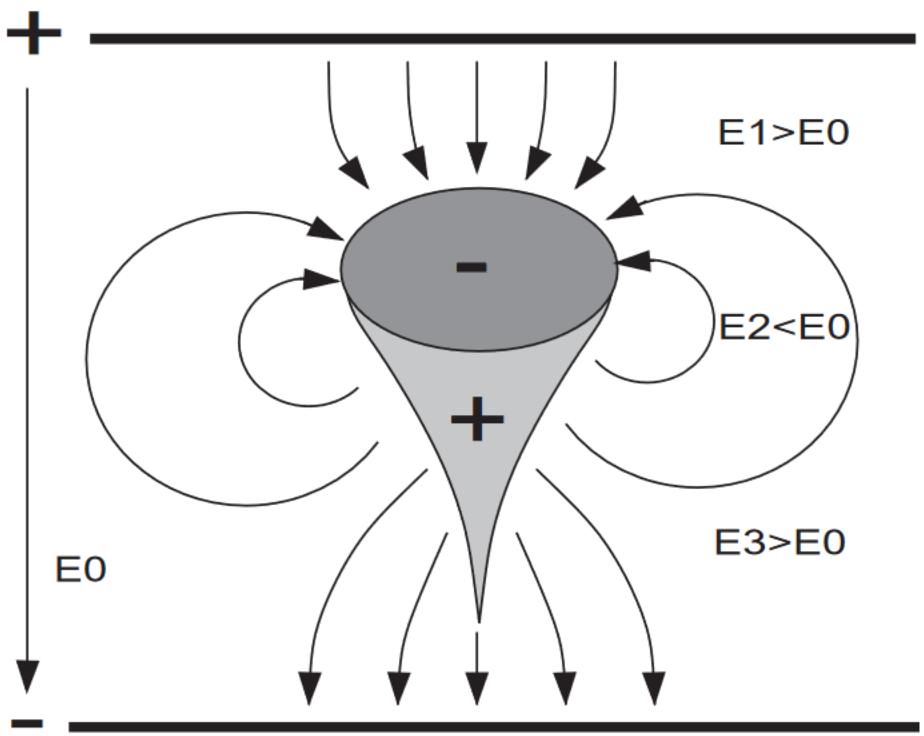

DLCスパッタリング

- **スパッタリング法**
  1. 真空中で不活性ガス(主にAr)を添加する
  2. 蒸着材料に負の電荷を与える
     ➔ グロー放電を起こし、ガス原子をイオン化
  3. ガスイオンを高速でターゲットに衝突させる
  4. 叩き出されたターゲット構成粒子が
     基板表面に付着・堆積
     ➔ 薄膜を形成

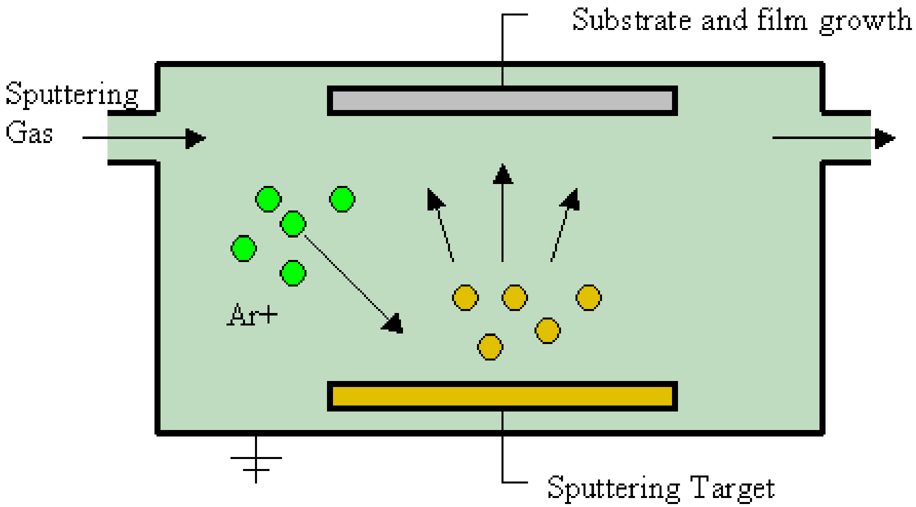

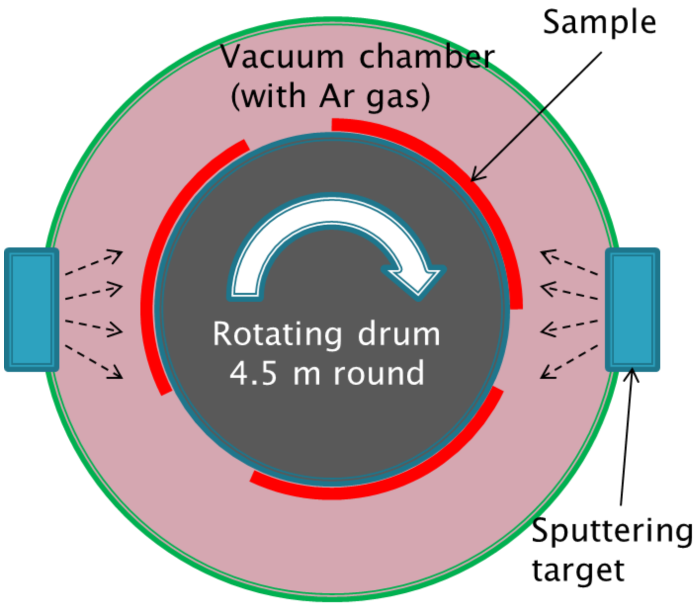

フォトレジストの取付

1. マスクをかけて
UV光で露光する

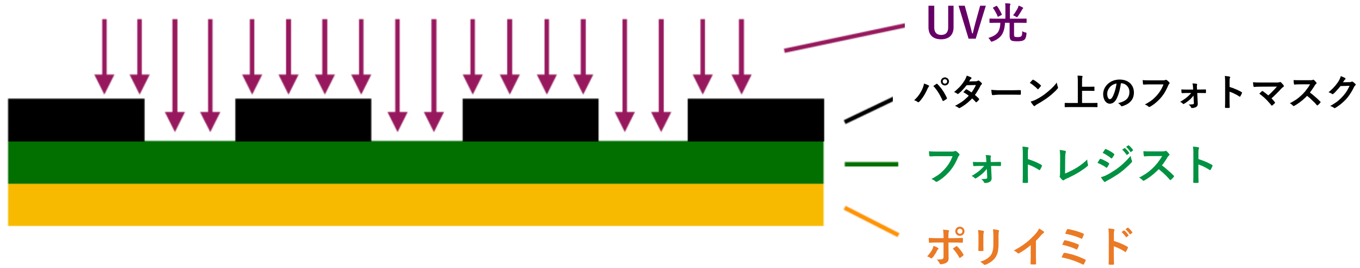

2. 現像液によって
非露光領域を溶かす

3. ピラーが完成する

MEG II実験 DLC-RPCのデザイン

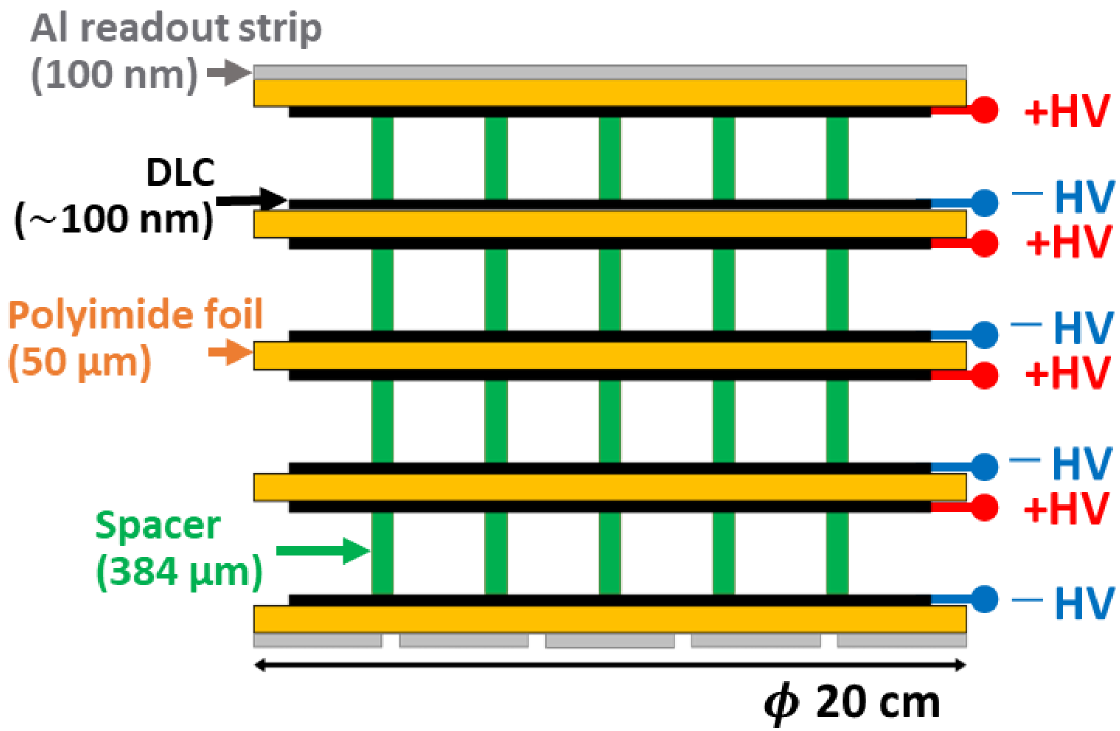

検出器素材	物質量
ポリイミド 50 µm	0.0175% X_0 [51]
アルミニウム 30 nm	0.0034% X_0 [51]
ガス 2 mm	~0.001% X_0

DLCの物質量は無視できる

先行研究における検出効率

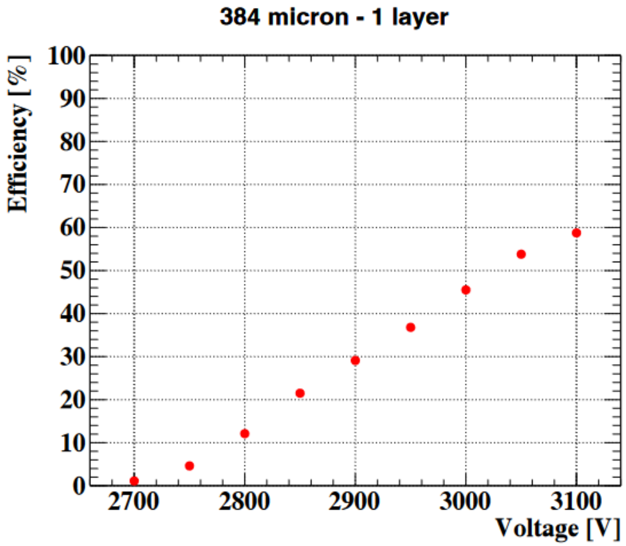

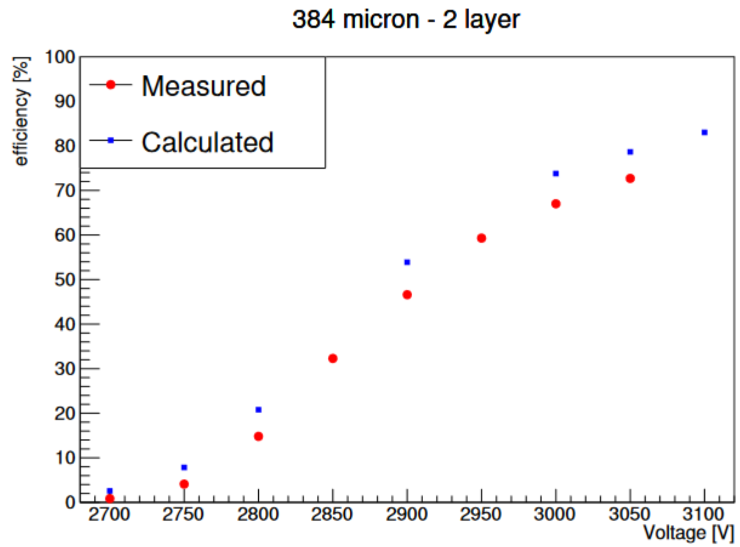

Calculated by
$\epsilon_n = 1 - (1 - \epsilon_1)^n$

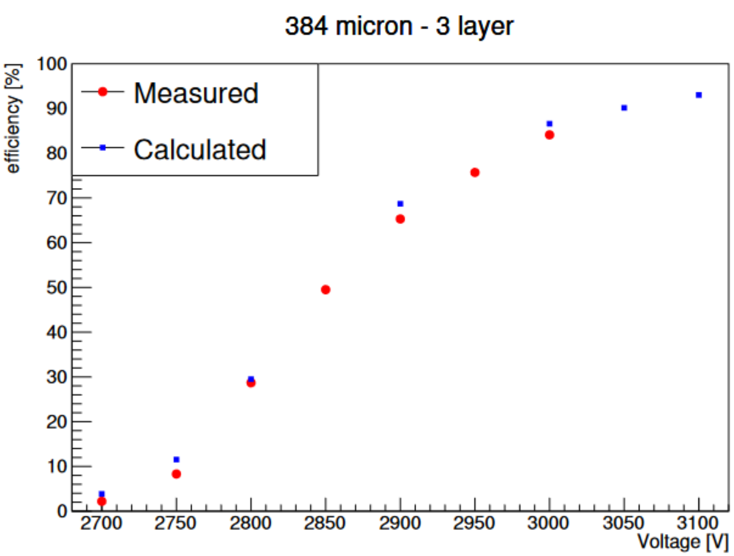

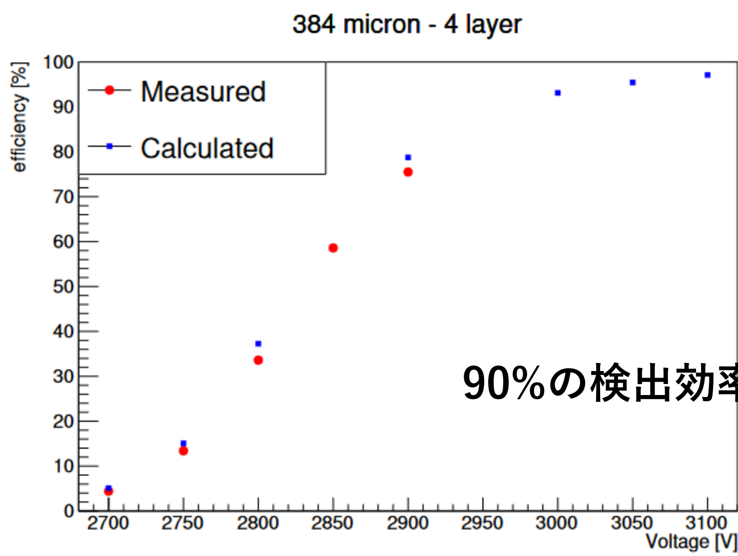

90%の検出効率が達成見込み

先行研究における時間分解能

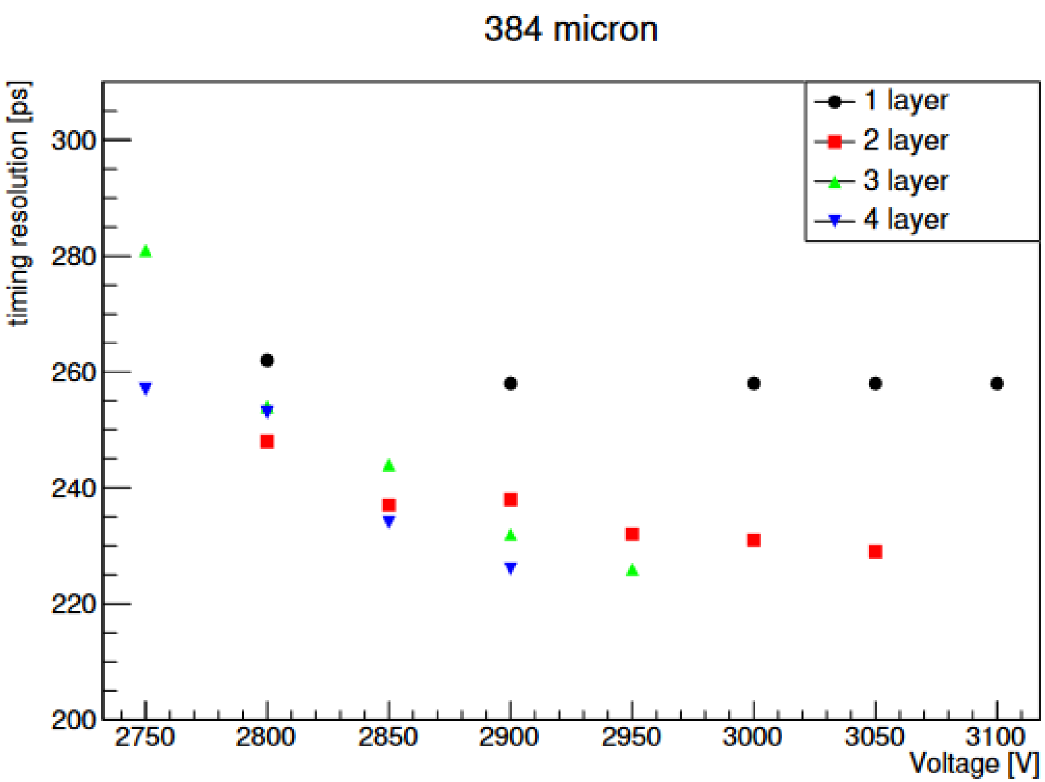

1 ns 以下の時間分解能を達成
(リファレンスカウンタなどの測定系の寄与も含む)

使用した増幅器

- 38 dB (80倍) の増幅器

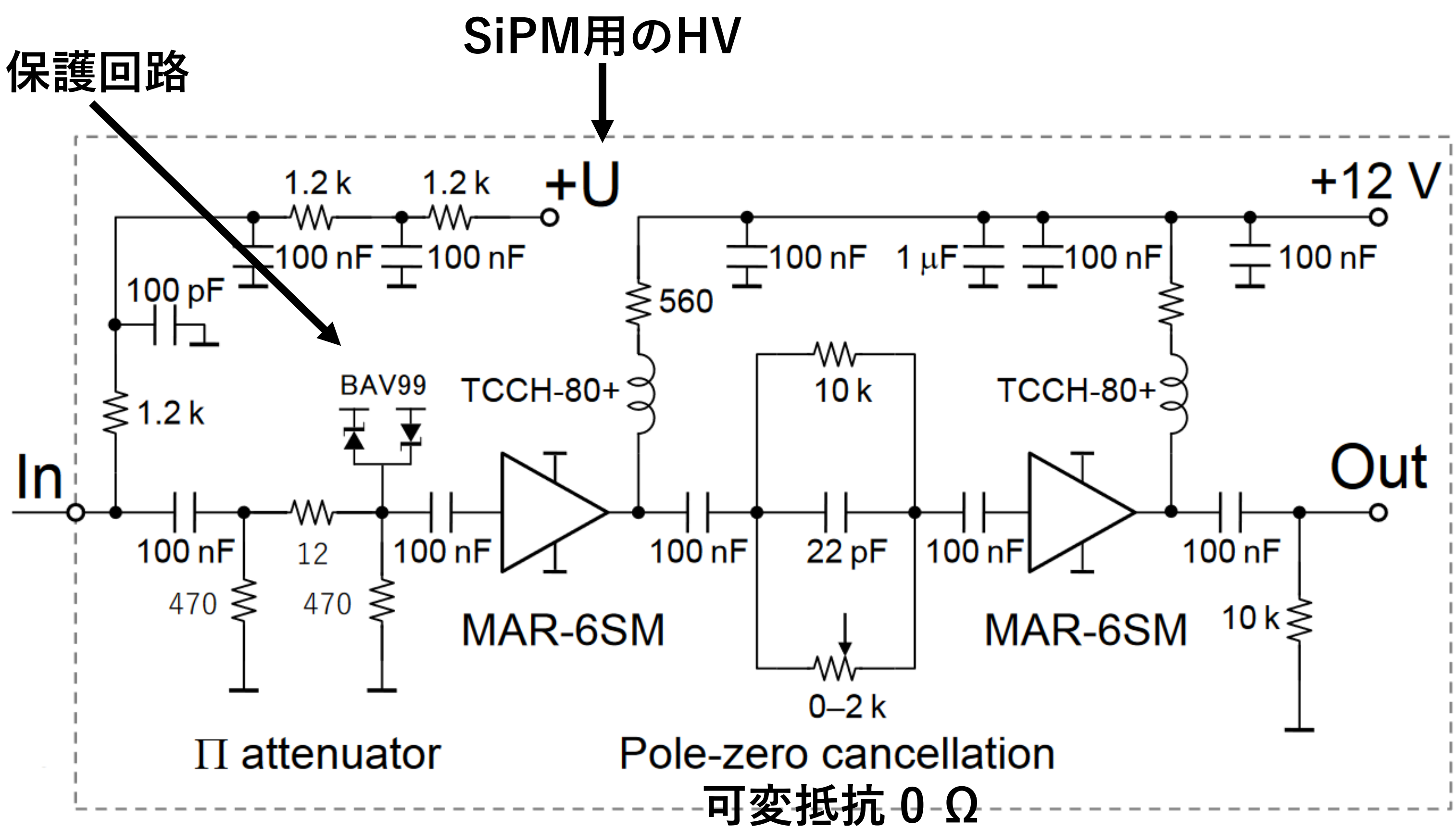

中性子照射中の検出器の状態

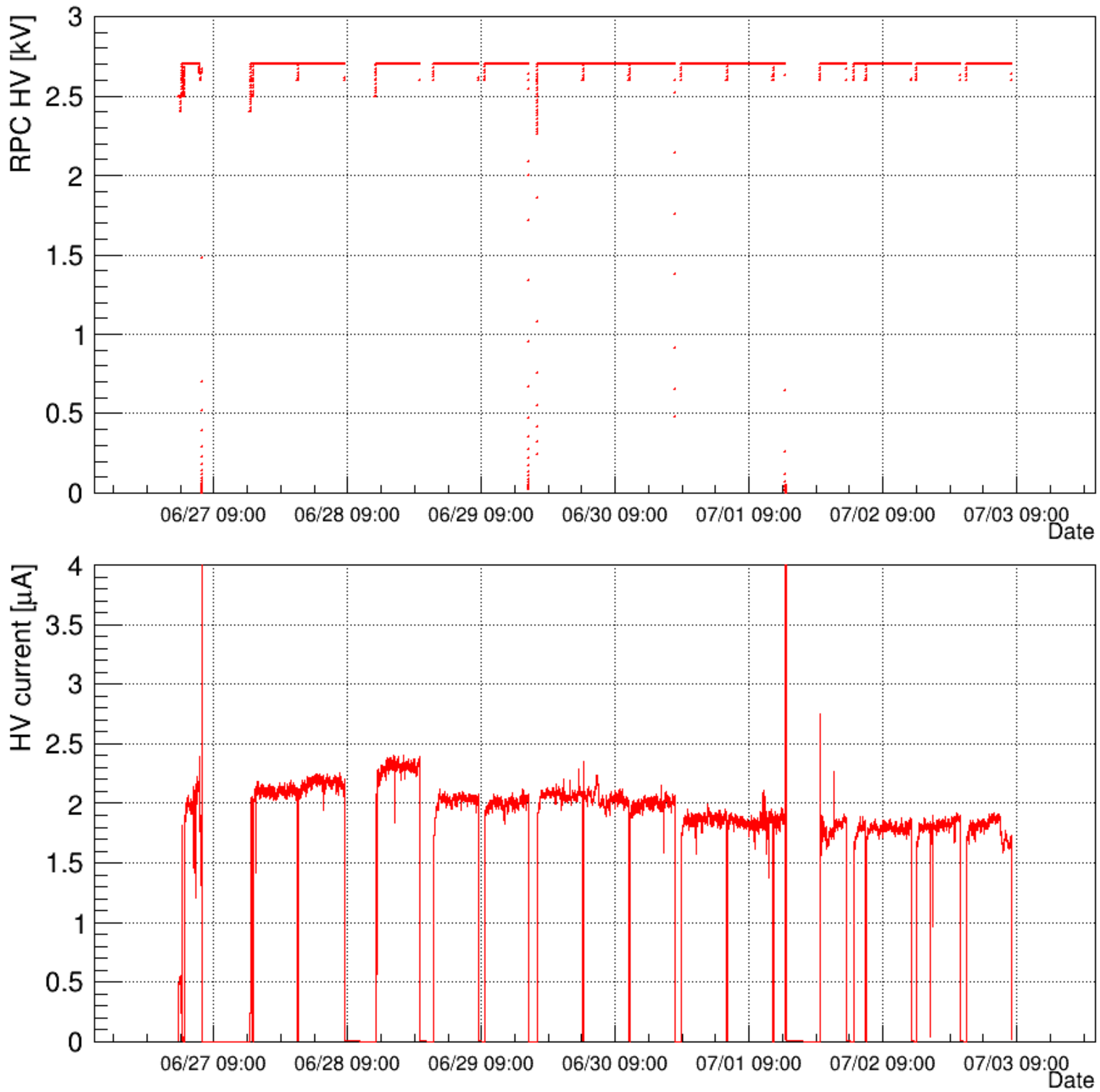

中性子照射中のビームカレント

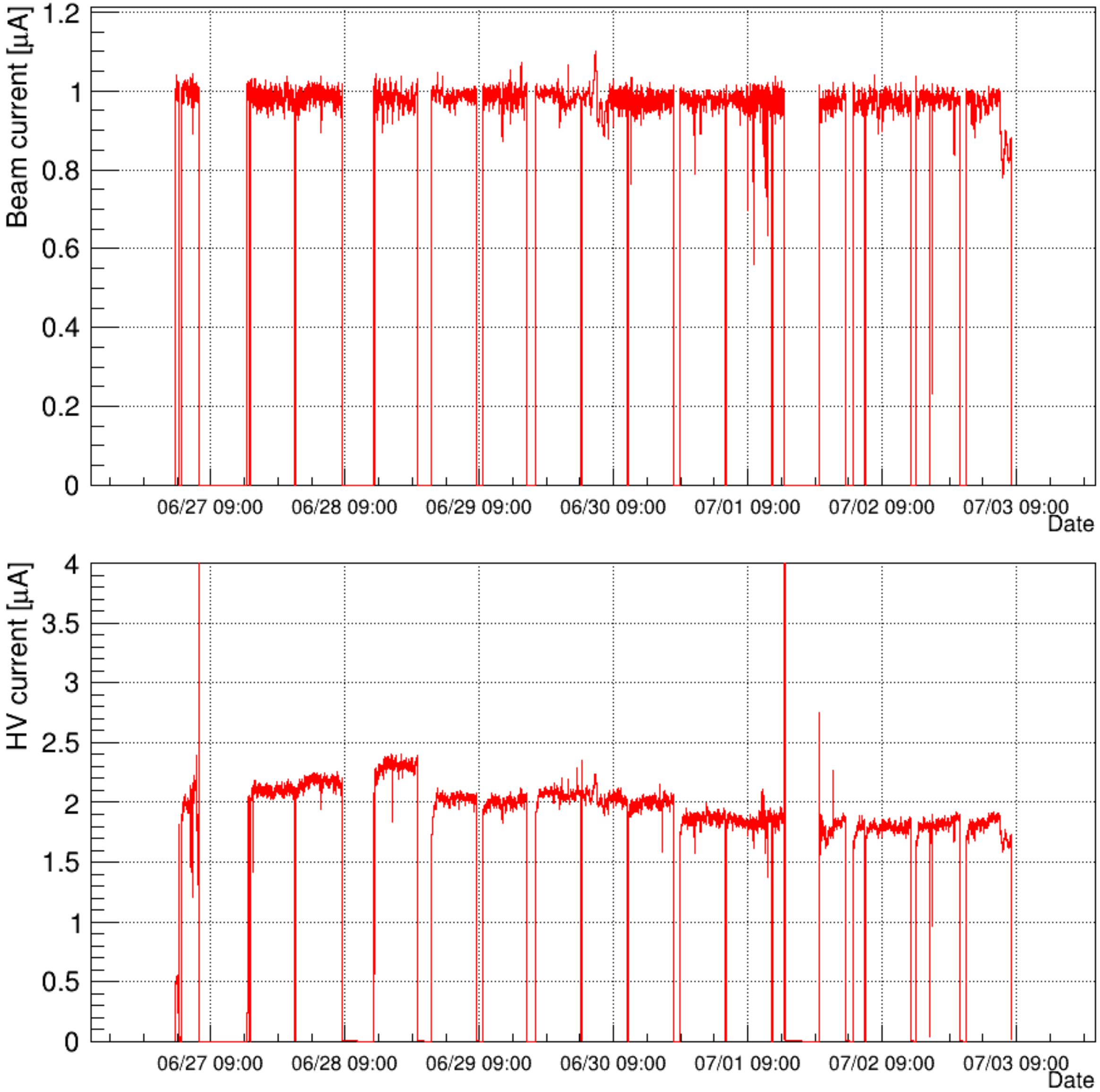

X線照射位置

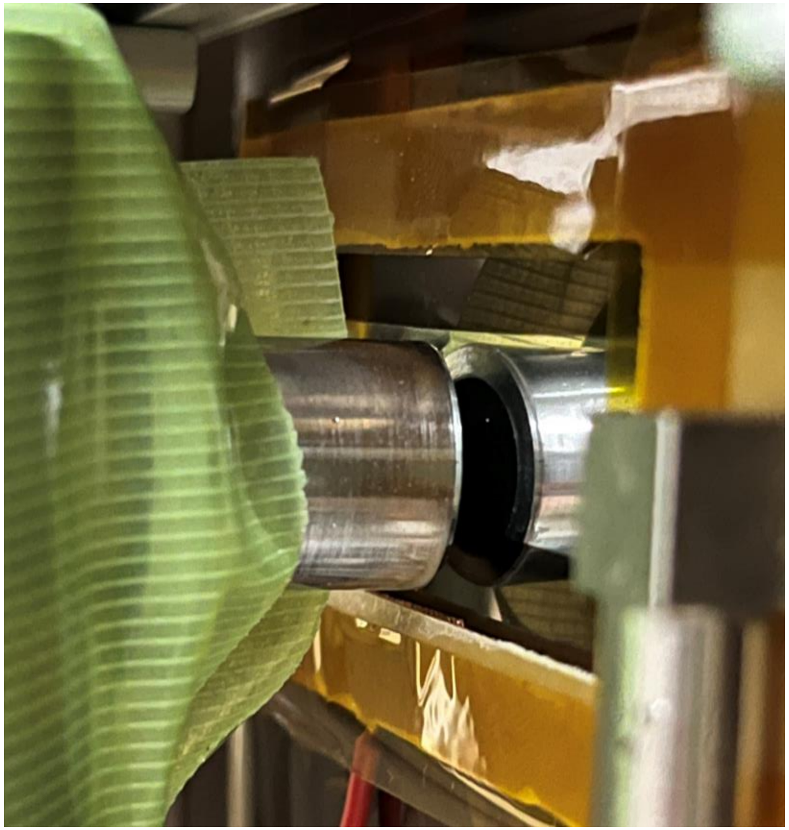

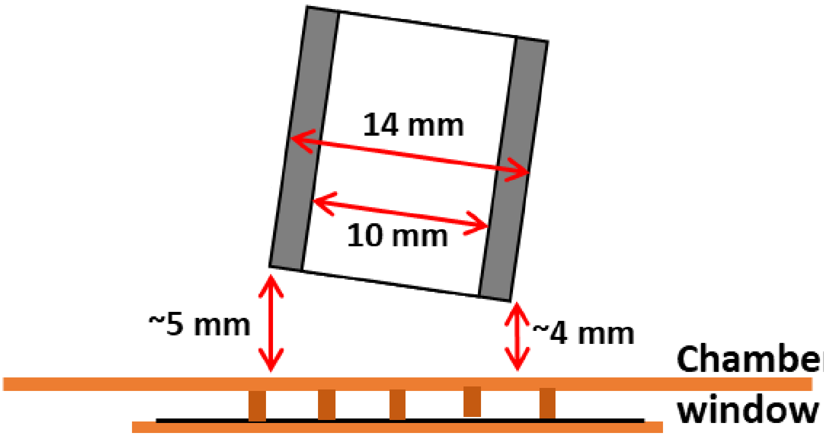

Incidence angle : ~ 4-5 degrees

X線照射中のDLC-RPCの状態

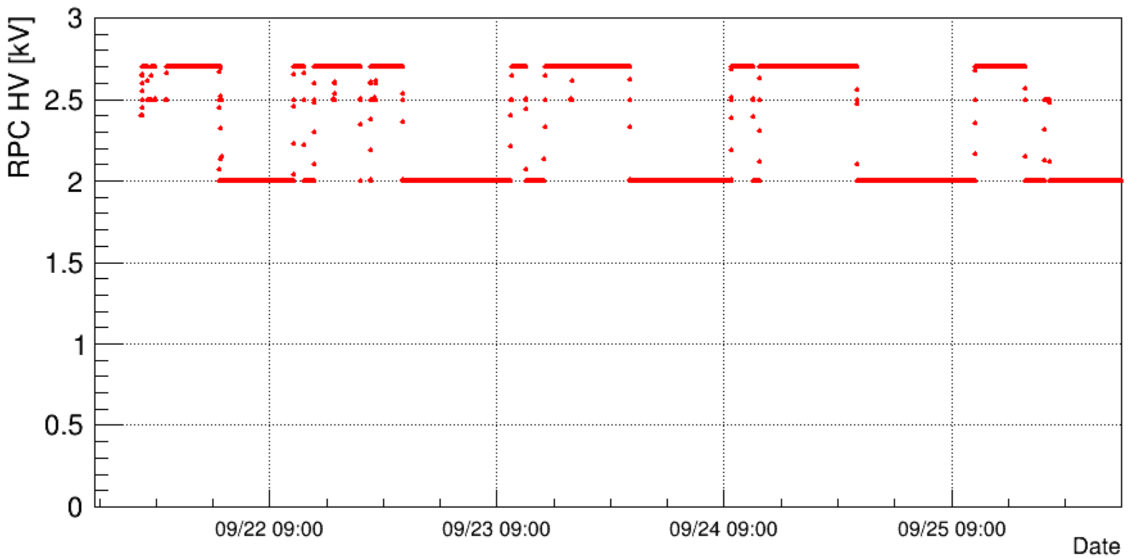

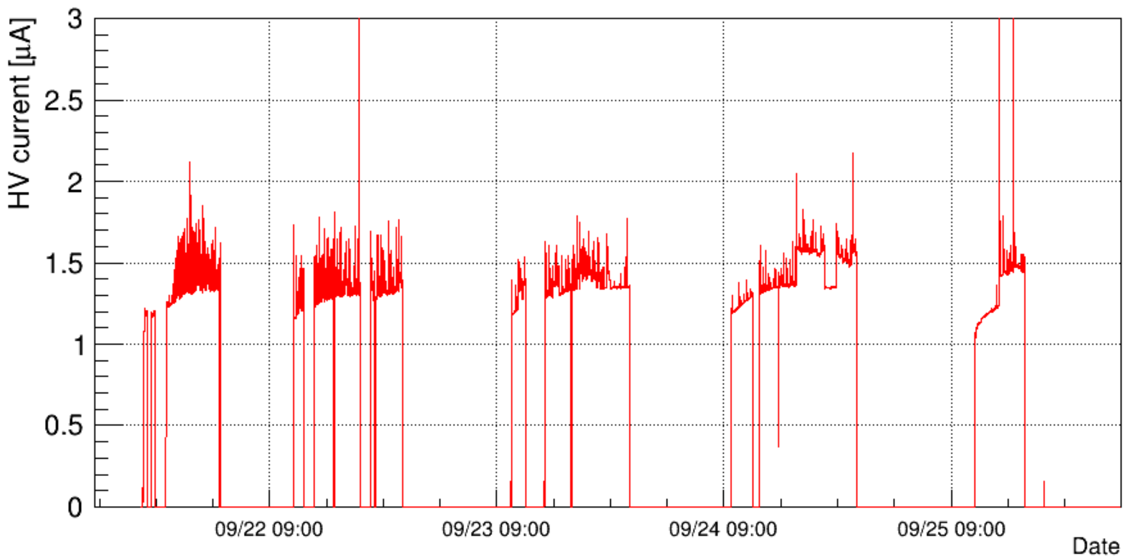

X線に対する波高分布

XG: 20 kV, 2 mA

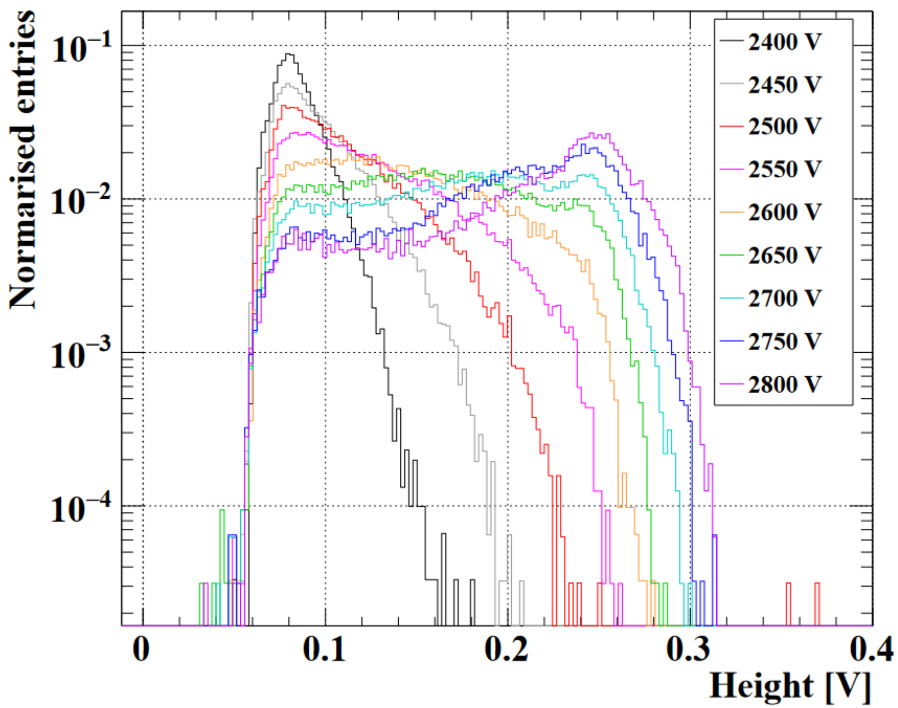

DLC-RPC: 2.8 kV, XG: 50 kV

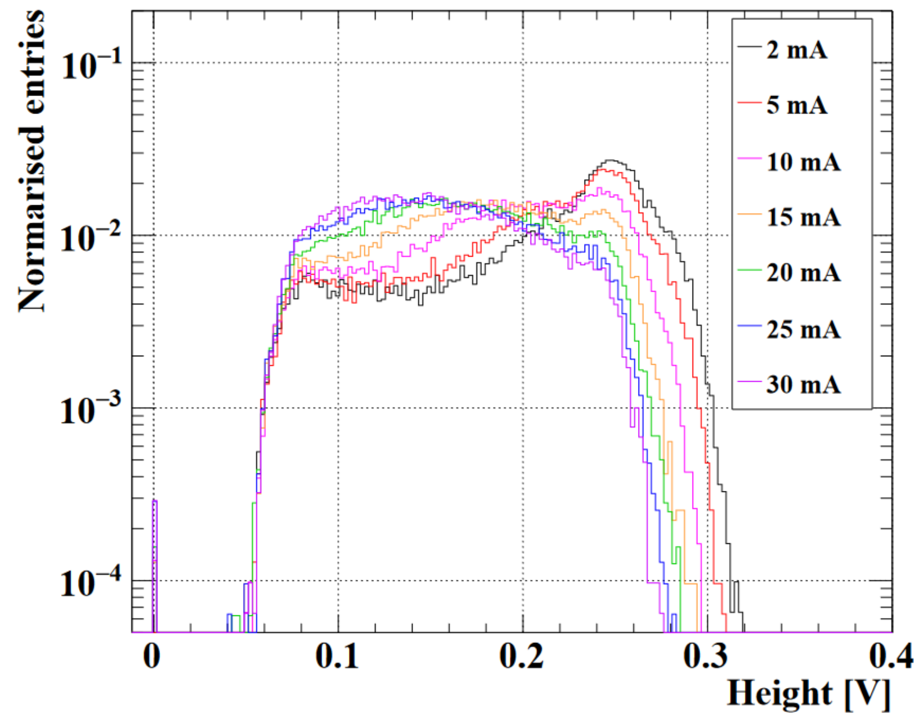

X線照射中の電流値変化

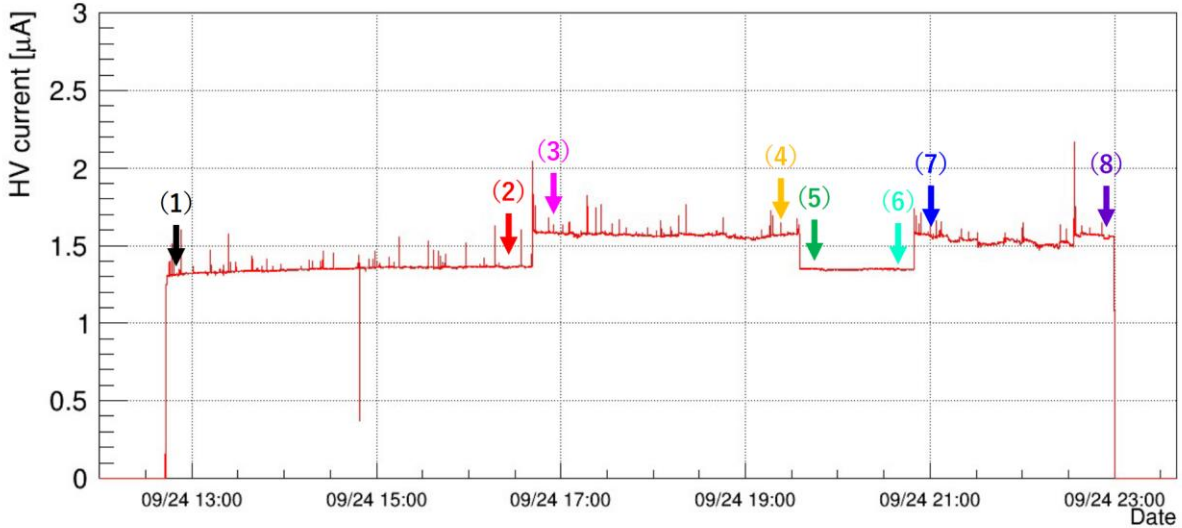

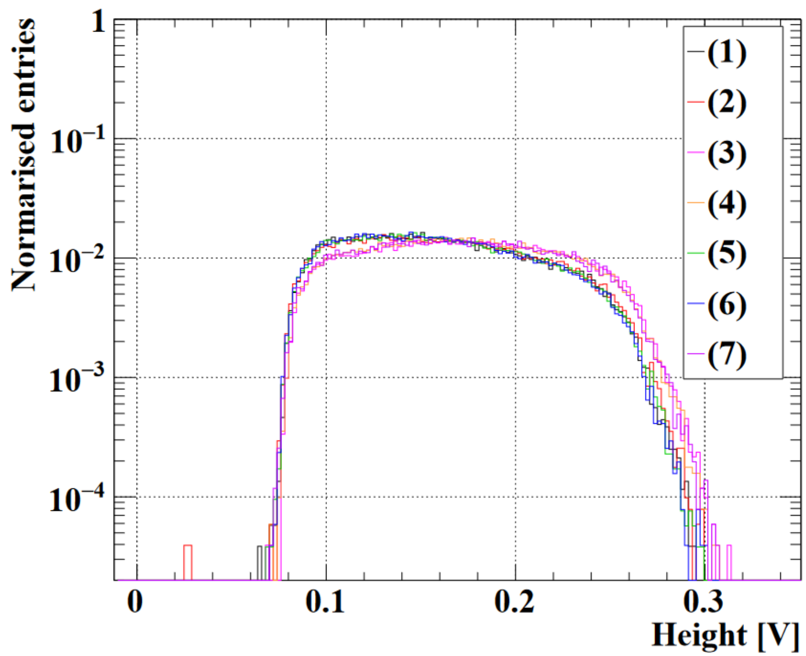

各電極サンプルの元素組成割合

電極サンプル	C1s(%)	N1s(%)	O1s(%)	F1s(%)	Si2p(%)
Non-irradiation	79.03	3.19	17.78	–	–
Neutron irradiation （active region）	76.06	–	15.22	7.37	1.35
Neutron irradiation （inactive region）	72.82	3.02	19.72	1.53	2.91
X-ray irradiation （anode discharge point）	67.63	–	15.52	14.51	2.35
Cathode active region	74.82	–	17.22	5.89	3.68
Cathode inactive region	81.20	–	15.72	–	2.37